

DESIGN OPTIMIZATION TECHNIQUES FOR IMPROVED POWER FACTOR AND
ENERGY EFFICIENCY FOR INDUSTRIAL PROCESSES

by

Darren R. Rabosky

© Copyright by Darren R. Rabosky, 2012

All Rights Reserved

A thesis submitted to the Faculty and Board of Trustees of the Colorado School of Mines in partial fulfillment of the requirements for a degree of Master of Science (Electrical Engineering).

Golden, CO

Date _____

Signed: _____

Darren R. Rabosky

Signed: _____

Dr. Pankaj K. Sen

Thesis Advisor

Golden, CO

Date _____

Signed: _____

Dr. Randy Haupt

Professor and Department Head

Electrical Engineering & Computer Science

ABSTRACT

Poor power quality such as reduced *power factor* and high levels of *harmonic distortion* create a number of problems for electrical utilities, and large industrial consumers are typically charged accordingly. Reduced *power factor* is such a common problem based on typical loads that techniques are frequently applied to improve *power factor* when it is below certain levels.

Traditional methods for improving *power factor* typically include adding *power factor* correction capacitors to supply the reactive volt-ampere reactive (VARs) near the location that inductive loads are absorbing VARs. In addition to inductive loads creating reduced lagging *power factor*, power electronic devices often reduce *power factor* similarly. Power electronic devices have become so commonly used that sophisticated techniques have been developed to improve *power factor* and reduce current *total harmonic distortion* for such devices. A common technique utilized for processes that must provide a large range of possible voltages is to include additional transformer taps coupled with the power electronic devices.

In addition to traditional methods for improving *power factor*, by careful consideration during the design phase of processes and load cycles that have a repetitive nature, *power factor* can be improved even further. Such a technique uses a computer algorithm approach to determine the ideal compromise of the relevant design parameters for improved energy efficiency and *power factor*.

TABLE OF CONTENTS

ABSTRACT.....	iii
LIST OF FIGURES	v
LIST OF TABLES.....	vii
ACKNOWLEDEMENTS	viii
CHAPTER 1 – INTRODUCTION AND BACKGROUND	1
1.1 Electrical power and energy delivery.....	2
1.2 Introduction to power electronics and non-linear loads	12
1.3 Traditional methods for improving power quality	17
CHAPTER 2 – A METHOD FOR FURTHER IMPROVING POWER FACTOR AND ENERGY EFFICIENCY FOR REPETITIVE PROCESSES OR LOAD CYCLES.....	24
2.1 Simplified example using energy efficiency for concept demonstration	24
2.2 Simplified example applied using power factor.....	28
2.3 Power factor improvement method applied to a repetitive industrial process.....	32
2.4 Design optimization summary	42
CHAPTER 3 – ECONOMIC EVALUATION	44
CHAPTER 4 – SUMMARY AND CONCLUSIONS	48
4.1 Future Work.....	50
REFERENCES CITED.....	51
APPENDIX A – MATH MODEL DEVELOPMENT	54
APPENDIX B - EXPERIMENTAL MEASUREMENTS AND MATH MODEL VERIFICATION.....	65
APPENDIX C - HARMONIC CANCELLATION.....	75

LIST OF FIGURES

Figure 1.1:	Total U.S. Energy in Quads of BTU [1]	2
Figure 1.2:	How electrical energy is delivered [2]	3
Figure 1.3:	Circuit with voltage, current and power relationships.....	5
Figure 1.4:	System with increased power losses.....	6
Figure 1.5:	Typical residential voltage waveform.....	6
Figure 1.6:	Phasor representation of AC voltage.....	7
Figure 1.7:	Lagging current displacement from voltage.....	9
Figure 1.8:	Household light dimmer circuit.....	13
Figure 1.9:	Light dimmer half dimmed (load side)	14
Figure 1.10:	Light dimmer dimmed to half power (90 degree firing)	15
Figure 1.11:	Power factor correction capacitor installation.....	18
Figure 1.12:	Light dimmer power factor vs. load RMS voltage	19
Figure 1.13:	Adding a second transformer tap at 60 volts.....	20
Figure 1.14:	Addition 60 volt tap included and used with the dimmer (load side).....	21
Figure 1.15:	Power factor for using a 60v and 120v taps	22
Figure 2.1:	Power flow and delivery	24
Figure 2.2:	Process load characteristics	25
Figure 2.3:	Power and reactive power delivery	29
Figure 2.4:	Example of an industrial process utilizing electrical heating.....	32
Figure 2.5:	Transformer utilized for resistive heating process control.....	33
Figure 2.6:	Transformer Design 1	34
Figure 2.7:	Transformer Design 2	34
Figure 2.8:	Required process information.....	35
Figure 2.9:	Algorithm flow chart.....	36
Figure 2.10:	Process example 1 power and voltage requirements.....	37
Figure 2.11:	Process example 2 power and voltage requirements.....	38
Figure 2.12:	Process with continuously varying conditions	40
Figure 2.13:	Transformer Design 3	40
Figure 2.14:	Industrial bus with 8 systems.....	42
Figure A-1:	Half a cycle for a primary voltage with peak amplitude “P”	55
Figure A-2:	Primary and secondary voltages with peak P, A and B respectively	56
Figure A-3:	Transformer secondary/load voltage.....	57
Figure A-4:	Transformer secondary voltage with a lower tap of 0.....	58
Figure A-5:	Transformer primary current for a secondary load resistance of $R=1$	59
Figure B-1:	Experimental light dimmer setup	66
Figure B-2:	Supply current / voltage and load current / voltage	67

Figure B-3: Power factor for the dimmer half dimmed (90 degree firing)	67
Figure B-4: Light dimmer plot of power factor vs. RMS voltage	68
Figure B-5: Applied voltage, secondary waveform and fundamental harmonic.....	69
Figure B-6: Displacement power factors vs. firing angle	70
Figure B-7: Distortion factor vs. firing angle.....	70
Figure B-8: Power factor vs. firing angle	71
Figure B-9: Load voltage for 90 degree firing between 60 and 120 volt taps.....	72
Figure B-10: Power factor vs. RMS voltage operating between 60 and 120 volt taps	72
Figure B-11: Transformer primary and secondary currents for a 60 ohm load	73
Figure C-1: Transformer supplying an industrial load for process heating	75
Figure C-2: Industrial bus with several converter power supplies.....	76
Figure C-3: phase shift of the fundamental harmonic	77
Figure C-4: 3rd harmonic phase shift.....	78
Figure C-5: 3rd harmonic time domain for various firing angles.....	78
Figure C-6: 3rd harmonic and fundamental phasor displacement vs. firing angle. Note: different harmonics have a different angular speed of rotation.....	80
Figure C-7: 5th, 7th and 9th phase shift	81
Figure C-8: 3rd and 9th phase shift vs. firing angle.....	82
Figure C-9: Fundamental harmonic components for 3 systems.....	83
Figure C-10: 3rd harmonic component cancellation for 3 systems	83
Figure C-11: Delta connected primary phase winding current waveform	84
Figure C-12: Line currents for 3 systems simulated	85
Figure C-13: Sum of the line current for 3 systems	85

LIST OF TABLES

Table 2.1: Net energy consumed for process with 80% efficiency.....	26
Table 2.2: Net energy consumed for a more optimized design	27
Table 2.3: Real and reactive power required by the process load	29
Table 2.4: Time weighted real, reactive and apparent powers	30
Table 2.5: Real and reactive power for optimized design.....	31
Table 2.6: Time weighted average of real, reactive and apparent power	31
Table 2.7: Algorithm results for different center tap configurations.....	37
Table 2.8: Algorithm results for different center tap configurations.....	39
Table 2.9: Transformer design 1, 2 and 3 average power factor.....	41
Table 3.1: Example power factor fee schedule	45
Table 3.2: Transformer designs for economic comparison	46

ACKNOWLEDEMENTS

I would like to thank the faculty and staff at the Colorado School of Mines for the support, opportunities, and outstanding education provided to me as a funded thesis graduate student. I would specifically like to thank two instructors, Dr. Sen and Dr. Ammerman, who were instrumental in helping to refine and shape my education for their hard work to build an excellent energy and electric power program at the Colorado School of Mines. I would like to thank my thesis committee consisting of Dr. Rebennack, Dr. Ammerman, and Dr. Sen for their time commitment and for reviewing my thesis work. I owe a special thanks to my advisor Dr. Sen for the extra time he spent reviewing my thesis work, providing comments and suggestions. I would also like to thank my parents, Ron and Lynn Rabosky, for their continued support in all my endeavors. I also owe a thank you to my brother and sister-in-law, Dr. Dan Rabosky and Dr. Alison Rabosky, for their suggestions on my defense presentation. My final thank you is to my fiancé Dr. Kristin Kiriluk for her time spent reading my thesis providing additional suggestions and for the many hours she spent helping me resolve difficult formatting issues.

CHAPTER 1 – INTRODUCTION AND BACKGROUND

Among some of the world's largest energy consuming nations, the U.S. Energy Information Administration data and statistics identify the breakdown of dominant forms of primary energy sources in the U.S. are Petroleum (36%), Natural Gas (26%), Coal (20%), Renewable (including Hydro) (9%) and Nuclear (8%) of the total annual usage of 97.3 Quadrillion (Quads) British Thermal Units (BTU) [1]. With increasing concern of the dominant forms of primary energy usage being fossil fuel based and not being able to be replenished at the rate they are being used as well as concerns over environmental impacts, there have been substantial efforts made towards improving energy efficiency, increasing the percentage of renewables as well as exploring new ways of using energy. In addition to finding new ways to use energy, it is also important to utilize the existing systems in place in the most efficient manner possible. The focus of the research conducted in this document is towards determining the optimal design of existing electrical systems to use energy in the most efficient manner possible. It can be seen in Figure 1.1 that 40% of the total energy usage is for conversion to electric power [1], the majority which is lost during the thermodynamic conversion process. The remainder of the electrical energy is provided to the remote end users via high voltage transmission and distribution lines.

Electrical power transmission and distribution systems have a unique advantage of being able to convert energy from a primary energy source and transmit electrically over long distances to remote sites where it can be re-converted to mechanical energy (via electric motors), heat (via electric heaters) or other forms as desired by the end

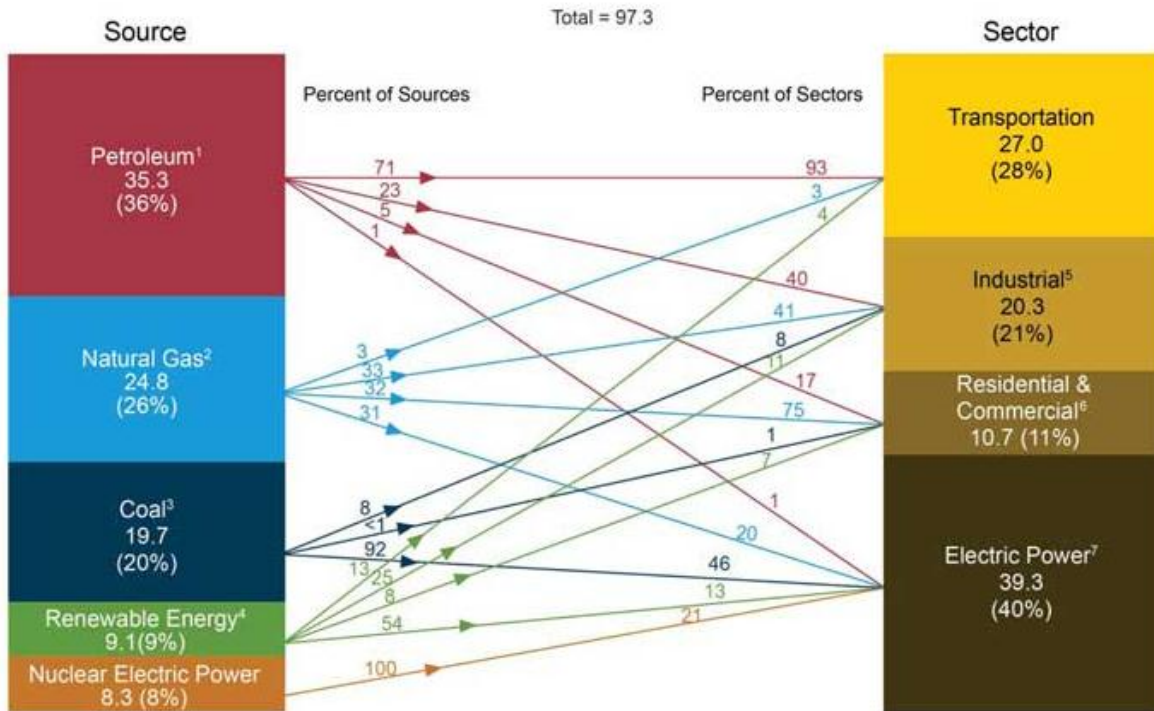


Figure 1.1: Total U.S. Energy in Quads of BTU [1]

user; residential, commercial and industrial. The end user utilizing the electrical energy must pay for the cost of the original fuel source and additionally must indirectly pay the capital costs of equipment, operational and maintenance costs to provide the energy, as well as losses incurred due to system inefficiencies. The general structure of the electrical generation, transmission and distribution system is shown in Figure 1.2 [2].

1.1 Electrical power and energy delivery

It is important to distinguish the difference between two commonly used terms, power and energy. A ton of coal, for instance, has a fixed amount of energy that can be used to produce heat and/or drive a mechanical system through a steam turbine.

Power is the rate at which the energy is used (energy/time). A system requiring twice as much power would use up the original coal source in half the time. In general, the end user is paying directly for the energy that they utilize but they indirectly pay for other aspects necessary to provide the energy as was discussed. These additional aspects include capital costs of equipment necessary for generation, transmission and distribution as well as labor and other indirect costs of reliably delivering the energy. The utility company charges the end user for electrical energy used in the units of kWh. One kW of power used for 2 hours is 2 kWh of energy. A typical utility charge for residential customers [3] is \$0.109/kWh. Using a round number of \$0.10 / kWh, the 2 kWh of energy usage would cost \$0.20.

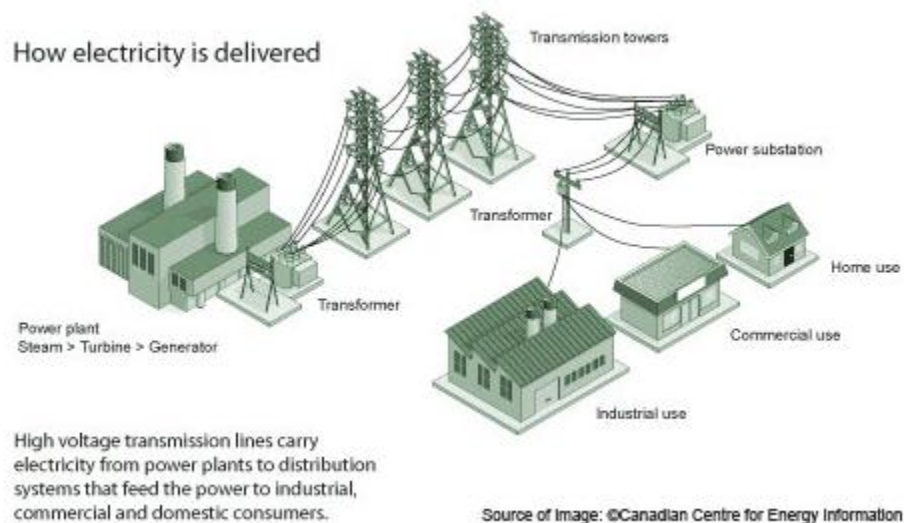


Figure 1.2: How electrical energy is delivered [2]

Generators are used to convert the original fuel source (coal, nuclear, hydro, etc.) to electrical power in the form of voltage and current. The product of the voltage and current is the electrical power being generated and is typically given in units of

Watts. One Watt is one Joule of energy used each second (J/s). Since a Watt is such a small unit of power, kilo-watts (kW) or Mega-watts (MW) are more commonly used terms when describing electric power. To reduce transmission losses and reduce line currents to a level practical for electrical conductors used for transmission, transformers at a substation are used to raise the voltage and reduce the current from the originally generated power. Energy and power must be conserved so any increase in voltage must result in a corresponding decrease in current. Near the end user, transformers are once again used to reduce voltage to a level practical for the end user (industrial, commercial, residential) to utilize. As the electrical power is transferred over long distances as well as each time transformations occur, some of the originally converted energy is lost from the system primarily in the form of heat but also mechanical vibration, sound, etc. Although the electrical utility is responsible for providing the power to the end user as efficiently as possible, once delivered, the end user pays for the energy they utilize including the energy lost due to inefficiencies from of how the end user utilizes the energy. For instance, an industrial plant using an electric heater will pay more on their energy bill for a less efficient heater than a heater that uses the energy more efficiently. Equations (1.1), (1.2) and (1.3) define voltage, current resistance and power relationships. As voltage is increased across a load resistor “R”, the power used is higher. A device that changes the voltage across a load resistance will also have some inefficiencies and some of the power supplied will be lost in the form of heat. An example circuit is shown in Figure 1.3 where the device changing the voltage does not need to be known, it can be considered a “black box”.

The current to the load and corresponding power used are higher when the voltage across the load resistor is higher. The power delivered to the load must equal the supply power less any system losses as is shown in the equation (1.3). If the system delivering power (i.e. raising or lowering the voltage) has reduced efficiency, the losses will be greater and the power at the load less as can be seen in Figure 1.4 compared to Figure 1.3.

$$I = V / R \tag{1.1}$$

$$P = VI = I^2R = V^2 / R \tag{1.2}$$

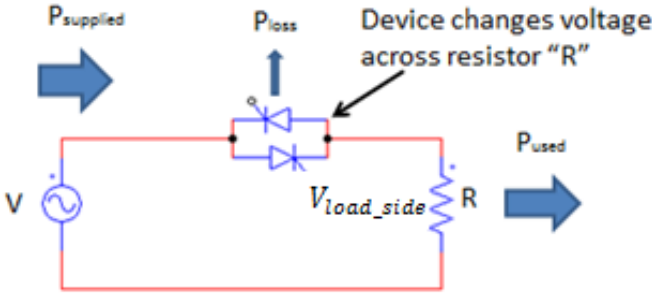


Figure 1.3: Circuit with voltage, current and power relationships

The definitions identified for voltage, current and power are straight forward for direct current (DC) systems. For an alternating voltage and current (AC) system, additional complications arise in how energy is transferred to the customer.

$$P_S - P_{loss} = P_U \tag{1.3}$$

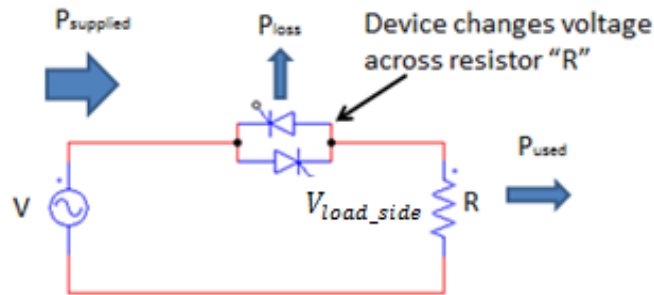


Figure 1.4: System with increased power losses

In an AC system, voltage and current oscillate in a sinusoidal manner repeating a cycle. For a frequency of 60Hz, the cycle time is approximately $T=16.67$ ms, where T is the time period for one cycle. An example for a typical residential house voltage is shown below where the peak voltage is approximately 170 volts.

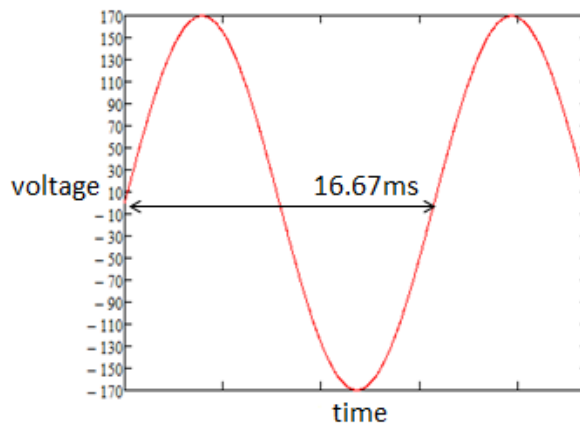


Figure 1.5: Typical residential voltage waveform

It is often more convenient to think of the AC voltage as a *phasor* where the length of the *phasor* represents the amplitude of the voltage. The *phasor* is imagined to be rotating in a circle and the projection on either the horizontal or vertical axis will represent the sinusoidal waveform amplitude at any instant in time. One complete rotation would represent one complete cycle or an angle of 2π radians in T seconds. A phasor representation of voltage is shown in Figure 1.6.

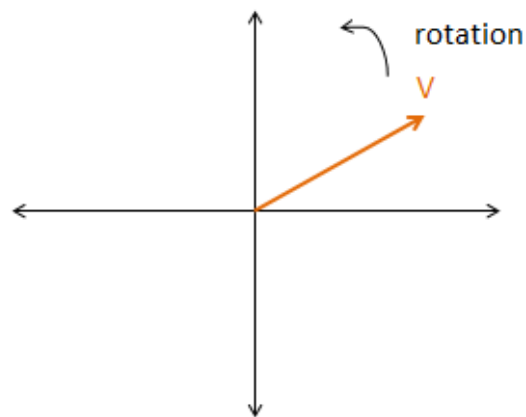


Figure 1.6: Phasor representation of AC voltage

In an AC system, power is still the product of voltage and current but it must be performed at each instant in time over the repeating cycle. When the voltage or current are 0, the power at that instant is also 0. Whereas when the voltage and current are both at a peak, the power is also at a peak or maximum value. Since the power constantly fluctuates in an AC system, the average power is what is important since it would result in the same equivalent work or heating as the net effect of the

instantaneous powers over a complete cycle. When describing voltage and current for an AC system, the *root mean square* (RMS) quantities as defined in equations (1.4) and (1.5) are used [4]. If the RMS voltage and current reach their peak and cross 0 at the same time, their product results in the power consumed. Whenever voltage and current are discussed in an AC system, it will be assumed the value discussed is the RMS value unless identified otherwise.

$$V_{RMS} = \sqrt{\frac{1}{n} \sum_{i=1}^n V_i^2} \quad (1.4)$$

$$V_{RMS} = \sqrt{\frac{1}{T} \int_0^T v^2(t) dt} \quad (1.5)$$

For the residential voltage waveform shown in Figure 1.5, the RMS voltage is only 120 volts even though the peak value was 170 volts. For AC systems, complications arise when the voltage and current do not peak and cross zero at the same instant in time. The term *apparent power* (S) is defined as the product of magnitude of the RMS voltage and current.

$$S = V_{RMS} I_{RMS} \quad (1.6)$$

Whenever there is a time difference between the peak or 0 cross values of voltage and current, the power related to energy usage is no longer the product of the

RMS voltage and current magnitudes. In the phasor diagram representation of voltage, the current can be thought to have an angular displacement from the voltage. When such a condition occurs, the power related to energy usage is defined in equation (1.7) where ϕ is the angular displacement of the current from the voltage on the phasor diagram.

$$P = V_{RMS} I_{RMS} \cos(\phi) \tag{1.7}$$

The cosine term is so commonly encountered that it is given its own name of *displacement power factor* as defined in equation (1.8). It is common to drop the *displacement* part of the term when talking about *displacement power factor* and simply identify as *power factor*. If such a simplification is performed, it can be assumed there are no harmonic currents (the terms will be further distinguished in section 1.2 when non-linear loads are introduced). The *power factor* is always less than or equal to one [5].

$$dpf = \cos \phi \tag{1.8}$$

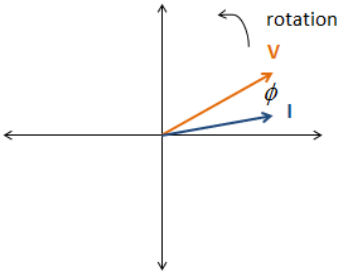


Figure 1.7: Lagging current displacement from voltage

The most common situations where the current is not perfectly in phase with the voltage is for inductive and capacitive loads. In inductive loads, energy is stored in the magnetic field and then return to the source. In capacitive loads, the energy is stored in the electric field and then returned to the source. In the case of inductive loads, the current lags behind the voltage by 90 degrees and in the case of capacitive loads, the current leads the voltage by 90 degrees. Inductive and capacitive loads tend to counter balance one another and can be used to bring the current in phase with the applied voltage. When the current is intentionally corrected to be in phase with the voltage, it is called *power factor correction*. For inductive and capacitive electrical loads, it was mentioned that the power is supplied to the load and then power is supplied from the load back to the source. This reactive interaction between the source and load is called *reactive power* and is defined by the quantity Q in equation (1.9).

$$Q = V_{RMS} I_{RMS} \sin(\phi) \quad (1.9)$$

The real power P, reactive power Q and apparent power S are orthogonally related by three sides of a right triangle in the mathematical relationship shown in equation (1.10).

$$S^2 = P^2 + Q^2 \quad (1.10)$$

The quantities for real power P, reactive power Q and apparent power S were defined for single phase AC power. More commonly, power is supplied and utilized as three phase and the above formulas are modified by a $\sqrt{3}$ multiplication factor and current and voltage are taken to be the line RMS quantities. The three phase apparent

power is shown below where the RMS subscript is dropped and considered to be understood.

$$S_{3\phi} = \sqrt{3}V_L I_L \quad (1.11)$$

One conclusion that can be drawn from the apparent power equation is that the line current is directly proportional to the apparent power. Additionally, the apparent power is related to the real power and *power factor* from the equation (1.12). A *power factor* of less than 1 increases *apparent power* and the corresponding line currents from the utility, decreasing the utility transmission, and distribution efficiency. The utility must also use larger equipment to handle the increased power levels.

$$S = P / pf \quad (1.12)$$

Since utilities charge for energy usage based on real power P over a given amount of time so it may not be immediately obvious to the end user why they may care about *power factor* and how that might affect the charges they receive from the utility company. As was discussed, since line currents must be higher for reduced *power factor*, the utility incurs higher energy losses in transmission. Additionally, as discussed, the utility must size generation, transmission and distribution equipment based on apparent power, all of which lead to increased costs for the utility. Utilities also have additional obligations when supplying power reliably to the end user. For instance, the utility is required to maintain a voltage of between 95%-105% of a nominal specified level (i.e. 120 volts for residential homes). The term % *voltage regulation* is used to identify how well the above goal is achieved. *Reduced power factor* from end users

tends to result in poor *voltage regulation* for the utility, requiring them to install expensive equipment to ensure desired limits are met. Since the above problems associated with reduced *power factor* result in increased costs to the utility, the end user is typically surcharged for reduced *power factor* and the costs can be significant (on par with charges for real power and energy usage [6]). Reduced *power factor* is one facet of a much larger category of issues identified by the term *power quality* that can result in indirect costs from the electric utility.

1.2 Introduction to power electronics and non-linear loads

Note: All mathematical model development and verification for results that are not specifically derived in this section are contained in the Appendix.

In the examples identified in Figure 1.3 and Figure 1.4, it was identified that changing the voltage across a resistor can be used to control the power consumed by the resistor. Changing the voltage across a resistive heating element is commonly referred to as *resistive heaters* in the process industries. The voltage can be changed by a number of methods including mechanical on-load tap changers where the turns ratio of the transformer is adjusted by the changing tap connections by mechanical switching. On-load tap changing can also be performed by power electronic devices [7]. Power electronic devices are often used to provide the function of changing the voltage because they have very low energy losses [8]. Additionally, if a continuous range of output voltage is required, power electronics devices can be used to provide such control. A common device using power electronics to change the voltage across a resistor and control how much power is consumed is a common household light

dimmer. A light bulb filament is a resistive heating element intended to reach such a high temperature that in addition to heat generated by the resistor, energy is also lost from the circuit in conversion to visible light. More power to the bulb yields a brighter bulb and vice versa. The common household light dimmer circuit shown in Figure 1.8 will be used to further define some of the additional relevant terms that may result in increased costs for large industrial consumers and/or are related to reduced *power factor*.

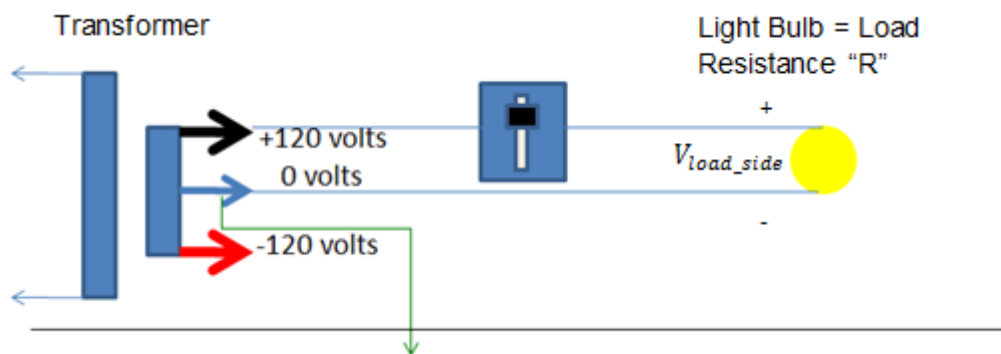


Figure 1.8: Household light dimmer circuit

The household light dimmer typically uses a Silicon Controlled Rectifier (SCR) switch to restrict or allow current to pass to the load. The SCR can be thought of as a switch that will turn on (allow current to pass to the load) when a pulse signal is sent to its gate and will continue to conduct until the current reaches 0 (zero cross). A second SCR switch is required for the reverse cycle. A pulse is sent to the pair of SCRs during each half of the cycle allowing it to turn on for both the forward and reverse cycles such that the voltage, current and power are precisely controlled to the light bulb. The sending of a pulse to the SCR is frequently called *firing angle* ϕ [8] and the term will be used to identify how early/delayed the SCR is sent a pulse. A firing angle $\phi = 0$ degrees

would correspond to the SCR conducting at the beginning of each half cycle, corresponding to a sinusoidal supply to the bulb. A 90 degree firing corresponds to a pulse being sent when the supply voltage is a peak. Adjusting the position of the dimmer switch controls the firing angle of the SCRs.

If the dimmer is in the brightest or full power position (approximately 0 degree firing angle), the voltage across the light bulb would be approximately sinusoidal as well as the current. It should be noted that there must be some small delay after the current reaches 0 and the firing angle cannot be 0 degrees, however, it can be maintained sufficiently small to be approximated as such. With the light dimmer in the half dimmed configuration, pulses are sent to the SCR's when the supply voltage is at a peak (90 degree firing). Almost instantly, the SCR conducts and remains conducting until the 0 cross. On the reverse cycle, a pulse must be sent to the SCR again at peak voltage. The resulting waveform is a chopped sine wave. Since the load is purely resistive, the current waveform will be exactly in phase with the load voltage and is simply the voltage divided by the current [9, 5, 10]. The resultant plot of the load voltage can be seen in Figure 1.9.

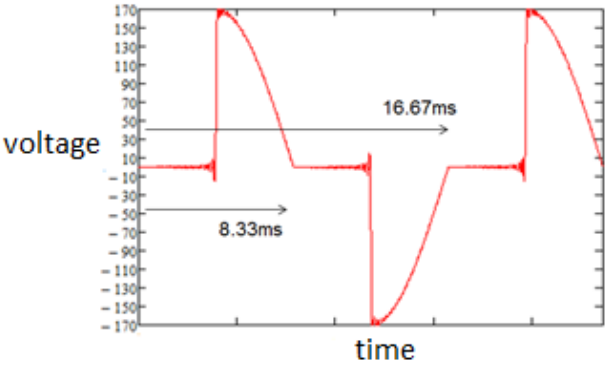


Figure 1.9: Light dimmer half dimmed (load side)

As derived in Appendix A using Fourier series, the resulting voltage waveform at the load can be expressed as a sum of sinusoids of integer multiples of the fundamental power system frequency (i.e. 60 Hz) [11]. Assuming a symmetric load waveform, the sinusoids include a component at the power system frequency (fundamental harmonic, $n=1$) and components with frequencies that are odd multiples of the power system frequency ($n=3, 5, 7, \dots$) [5, 11]. A plot of the fundamental, 3rd and 5th harmonics are shown in Figure 1.10. It can be seen from the plot that the fundamental harmonic has a time lagging displacement from the supply voltage similar to an inductive load. Since the current at the resistive load is in phase with the load voltage, this lagging displacement results in a reduced *displacement power factor* [5].

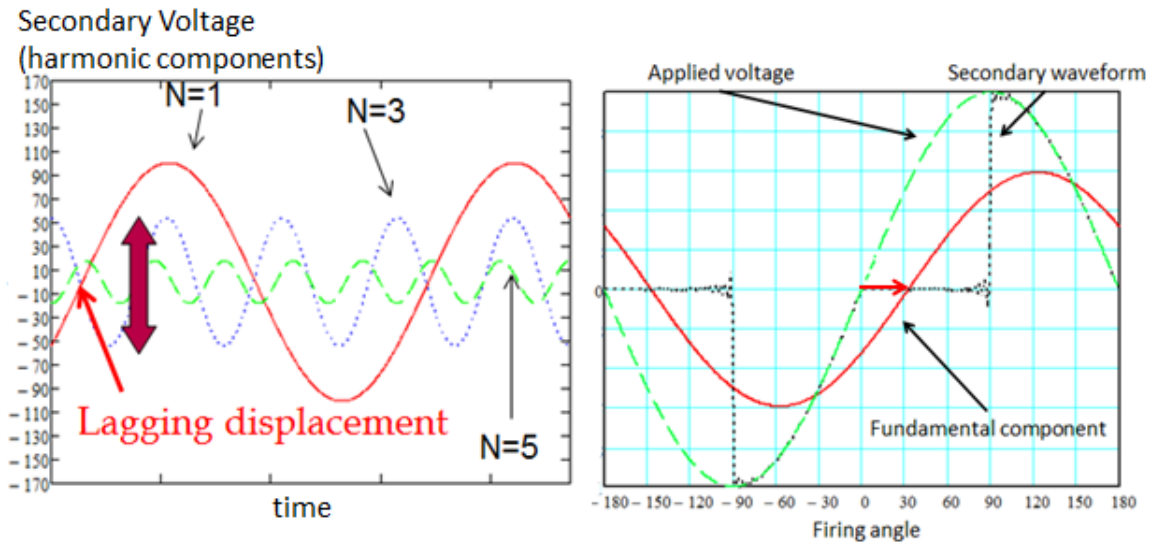


Figure 1.10: Light dimmer dimmed to half power (90 degree firing)

A commonly defined term to identify the amount of distortion in the current waveform is *Total Current Harmonic Distortion (THD_I)*. THD_I is the ratio of total RMS

current beyond the fundamental to the fundamental component and is defined in equation (1.13) [5].

$$THD_I = \frac{\sqrt{\sum_{n>1}^{n_{max}} I_n^2}}{I_1} \quad (1.13)$$

The harmonic components also result in a net reduction in *power factor (pf)* and their contribution is accounted for in the term defined *distortion factor (df)*. *Distortion factor* is defined in equation (1.14) and the quantity is always less than or equal to one [5]. The total *power factor* which is commonly called *true power factor (pf)* is the product of the *displacement power factor* and *distortion factor* as is shown in equation (1.15) [5]. For electrical devices that control current in such a manner that the current is no longer sinusoidal, the term *non-linear load* is used. *Non-linear loads* have the negative side effects of increased harmonic currents and reduced *power factor*. It is important to realize that the supply side of the dimmer where the voltage was sinusoidal must still supply the distorted current waveform to the load. When defining the above power quality terms for a sinusoidal voltage source, the distorted current must be compared to the sinusoidal source voltage (i.e. displacement of the fundamental component of current from the voltage results in the reduced *displacement power factor*) [5] [12]. For instance, if measuring *power factor* on the load (light bulb) side of the light dimmer circuit, the *power factor* would measure as 1 whereas on the supply side of the dimmer where the voltage is sinusoidal, the *power factor* will be less than 1.

$$df = \frac{1}{\sqrt{1+THD^2}} \quad (1.14)$$

$$pf = dpf \cdot df \quad (1.15)$$

A common phenomena known as *skin effect* is where AC current tends to have a higher current density near the surface of a conductor than towards the center. Such a re-distribution of current increases the effective resistance of the conductor, increasing system losses [13]. Skin effect is more pronounced at higher frequencies, therefore harmonic currents tend to increase system losses beyond the increased losses associated with reduced *power factor* corresponding to increased current magnitudes. Harmonic currents also create voltage drops across system impedances which can distort the original sinusoidal supply voltage [14]. Distorted voltage can create a number of power system problems including torque oscillations and vibrations on electric motors, and increased heating that reduce the life of plant equipment [13, 15, 16]. Similar to charging an industrial consumer for reduced *power factor*, utilities may also charge an industrial consumer for high levels of harmonic distortion [17]. *Total harmonic distortion* and poor *power factor* are just a couple examples of problems captured by the umbrella term *power quality*.

1.3 Traditional methods for improving power quality

Note: All mathematical model development and verification that are not specifically derived in this section are contained in the Appendix.

For most industrial processes, magnetic inductive energy storage tends to create the reduced lagging *power factor* (i.e. motors, transformers, etc.) [18, 19, 20]. To correct the *power factor* to near unity, *power factor* correction capacitors are typically installed near the load as shown in Figure 1.11.

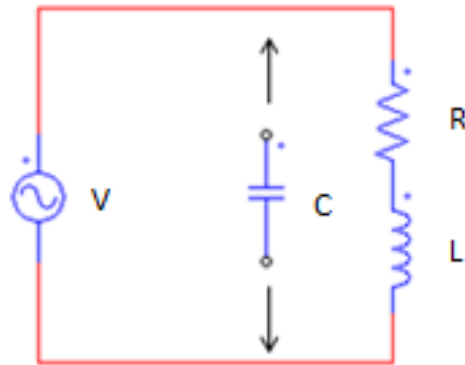


Figure 1.11: Power factor correction capacitor installation

Power factor correction capacitors tend to draw a leading current and therefore, correct the lagging current from the inductive loads. *Power factor* correction capacitors can only correct the *displacement power factor* and do not mitigate the harmonic currents and associated reduction in *power factor* due to *distortion factor*. *Power factor* correction capacitors are costly, require maintenance and ultimately have a shelf life [17] so it is more desirable to design the system to have a maximum *power factor* to begin with.

Returning to the household light dimmer and non-linear loads, a common technique used in industrial systems for improving *power factor* is examined. A plot of *power factor* vs. RMS voltage across the load (light bulb resistance) is shown for the

light dimmer in Figure 1.12 (derivations contained in Appendix A). From the plot, it can be seen that the *power factor* decreases linearly from 1 at the nominal tap voltage to a value of 0 at 0 volts. At the half power condition, the voltage at the load is $120/2^{0.5} \sim 85$ volts [8], where half power $P_{1/2}$ is shown to be $(120/\sqrt{2})^2/R = (1/2)(120^2/R) = (1/2)P$. The *power factor* can be seen to be approximately 0.71 for such a condition. The reduced *power factor* results in an increased line current of $1/0.71 \sim 1.41$, an approximate 41% increase.

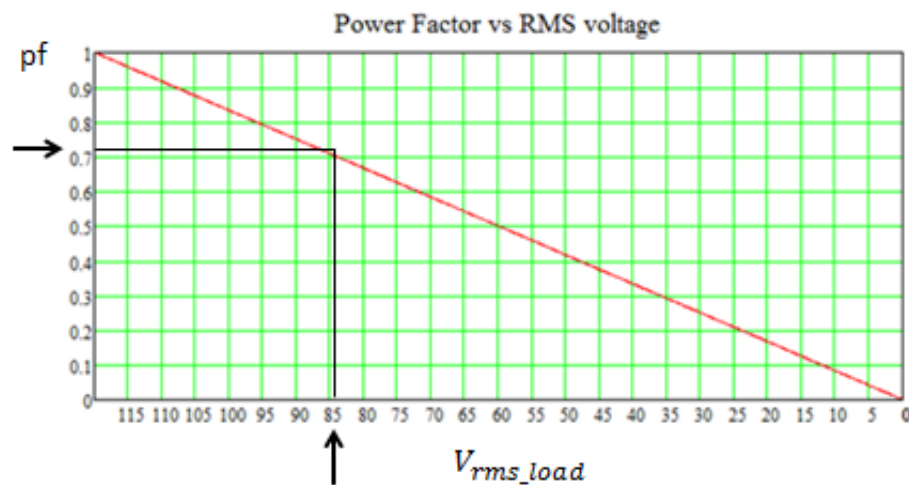


Figure 1.12: Light dimmer power factor vs. load RMS voltage

A method to have high *power factor* (near unity) and the ability to quickly change voltage levels is the use of solid state on-load tap changers using power electronic devices [7]. On-load tap changers work in conjunction with a transformer consisting of multiple transformer taps (as many taps as desired can be used considering practical design constraints) to apply transformer taps with different voltages across the load

through the switching of the power electronics. The voltage to the load would be applied in discrete steps determined by the transformer taps. In order to provide a continuously variable output voltage to a load, the electronic on-load tap changing methodology can be combined with firing angle control such as was used for the light dimmer. In such a configuration, the output voltage can be varied continuously between any pair of transformer voltage taps. Industrial power controllers utilizing electronic devices similar to the light dimmer often need to be able to provide a continuously variable output voltage and it is common to include additional voltage taps as described [17]. For the light dimmer circuit, a transformer tap has been added at 60 volts in addition the 120 volt tap as is shown in Figure 1.13. Such a waveform and associated harmonics are shown in Figure 1.14. Comparing the 3rd harmonic amplitude from Figure 1.10 shows a substantial reduction (purple arrow compared to the blue arrow). The reduction in harmonic currents results in an increased *distortion factor*. Additionally, the red arrow shown in Figure 1.14 identifies the original displacement of the fundamental harmonic before the addition of the 60 volt tap. As can be seen from the plot, there is a substantial reduction in the displacement of the fundamental component which results in an increased *displacement power factor*.

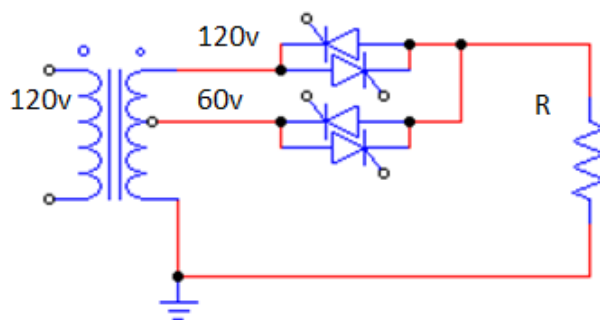


Figure 1.13: Adding a second transformer tap at 60 volts

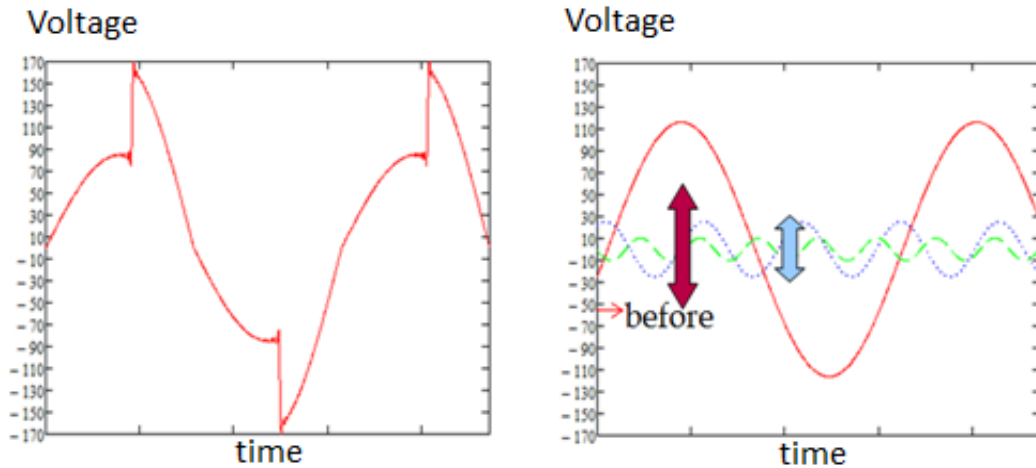


Figure 1.14: Addition 60 volt tap included and used with the dimmer (load side)

When adding the additional voltage tap, the *power factor* will have to approach 1 at either spectrum (firing angle adjusted to apply the lower voltage tap or higher voltage tap) since the supply would be sinusoidal at the nominal tap spacing. If a firing angle of 180 degrees were used, the output voltage would never change from the lower voltage tap to the higher voltage tap. A firing angle of 0 degrees on the other hand would correspond to an immediate control at the higher voltage tap level. Changing between 0 and 180 degrees would essentially function as an electronic switching on-load tap changer. Any firing angle between would provide a continuously variable output voltage as defined by RMS quantities derived in Appendix A. The plot for *power factor* vs. RMS voltage between the 60 and 120 volt taps is shown in Figure 1.15. Comparing to the plot in Figure 1.12, it can now be seen that the *power factor* never drops below 0.8 and the *power factor* is approximately 0.82 at 85 volts compared to the original *power factor* of approximately 0.71 when operating in phase angle control. If the lower voltage tap is

increased to a value greater than 60 volts, the minimum *power factor* between the pair of voltage taps will be even higher. Further evaluation, experimental data and discussion are included in Appendix A and B.

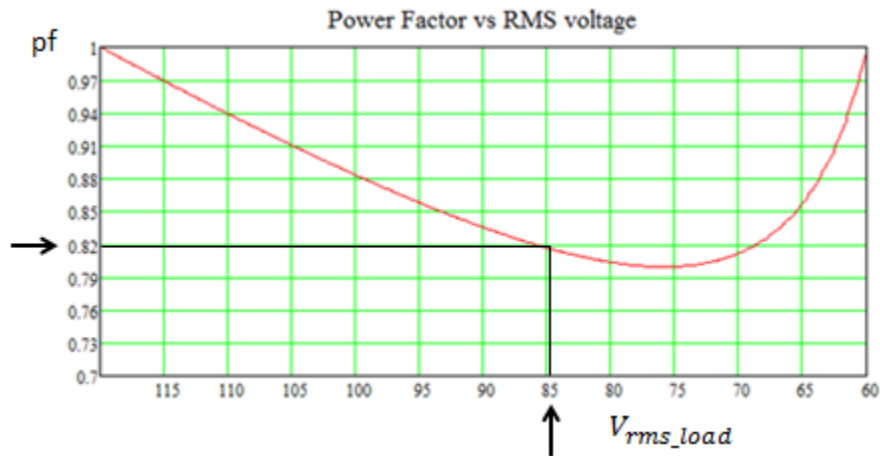


Figure 1.15: Power factor for using a 60v and 120v taps

The use of multiple transformer secondary taps and power electronics is commonly utilized in the process industries to provide precise process control with improved *power factor* and harmonic distortion [17]. There are many types of power electronic devices where similar techniques are employed depending on the design (i.e. Insulated Gate Bipolar Transistors, Gate Turnoff, Power Mosfet, etc. [8, 10, 21]).

Improving *power quality* such as improving *power factor* and reducing *total harmonic distortion* has many benefits, some of which are summarized below [18, 13, 20, 22, 14, 16].

- 1) Improve energy transmission efficiency by reducing system losses
- 2) Improve voltage regulation

- 3) Free system capacity
- 4) Improved system security
- 5) Decrease costs by reducing equipment size
- 6) Improved interchange transfer capability
- 7) Improved system operation
- 8) Increase the life of plant equipment
 - a. Reduce heat loading which degrades insulation life of plant equipment
 - i. Reduced *power factor* increases line currents increasing equipment size and increases transmission $(I^2)R$ losses
 - ii. Harmonic currents increase $(I^2)R$ losses through skin effect heating and additionally increase transformer core losses. Eddy current losses are proportional to frequency²
 - b. Voltage distortion within the plant associated with harmonic currents creating voltage drops across system impedances which are subtracted from the originally sinusoidal supply voltage can create problems for other plant connected equipment such as motors.

CHAPTER 2 – A METHOD FOR FURTHER IMPROVING POWER FACTOR AND ENERGY EFFICIENCY FOR REPETITIVE PROCESSES OR LOAD CYCLES

Note: All mathematical model development and verification for results that are not specifically derived in this section are contained in the Appendix.

When industrial process conditions or load cycles are batch (repetitive) or approximately repetitive, an approach different from the traditional methods already discussed is possible to further improve *power factor*. Before proposing the methodology for *power factor*, a more simplified example using energy efficiency as the variable to be improved will be utilized to demonstrate the general concept.

2.1 Simplified example using energy efficiency for concept demonstration

Recalling the energy efficiency discussions and the systems identified in Figure 1.3 and Figure 1.4, it can be seen that inefficiencies in system design will result in losses. The system is again shown in Figure 2.1 below.

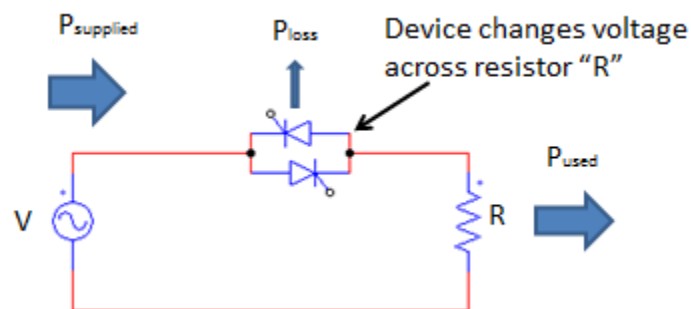


Figure 2.1: Power flow and delivery

Almost all design requires compromise of one sort or another. As an example, to have an improvement in efficiency for an electric motor at rated conditions usually requires a sacrifice elsewhere. Depending on the process characteristics, if it is desired to have a higher average efficiency for a range of operation, a design compromise may need to be made that reduces the efficiency at full loading [15]. An electric motor design is just one example of design compromise and almost all engineering system design requires such compromises to be made.

To demonstrate the general concept of utilizing design compromise for achieving a desired goal, assume the system shown Figure 2.1 is controlling a 3 hour industrial process requiring electrical power for heating with the following approximate load requirements outlined in Figure 2.2. It is not important to focus on the particular electrical design as was shown in Figure 2.1, the electrical system could be a motor driving a mechanical load, transformer, electric heater, etc.

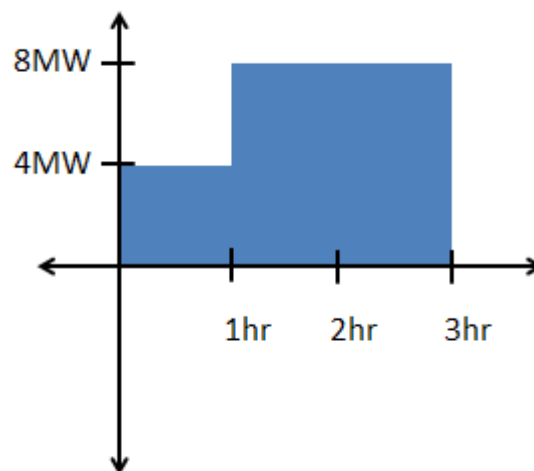


Figure 2.2: Process load characteristics

In the selection of equipment, the end user may have chosen the most efficient piece of equipment they can find to reduce operating costs related to energy usage. Assume the maximum efficiency for the range of possible conditions was a constant efficiency of 80%. It should be noted that the numbers used for efficiency in this section (2.1) have no physical significance as they are only utilized to demonstrate the general concept of design improvement through appropriate compromises. The 80% efficiency could have just as well been 85% for instance. Actual numbers will be utilized in section 2.2.

The total energy utilized for the process is calculated and the results shown in Table 2.1. As can be seen from the table, more energy is used during hours 2 and 3 due to the increased time as well as the higher power requirements during that portion of the process. Recall that power is the rate of energy usage.

Table 2.1: Net energy consumed for process with 80% efficiency

Energy consumed by load during hour 1	4 MWh
Energy consumed by load during hour 2 and 3	$8 \text{ MW} \cdot 2 \text{ hr} = 16 \text{ MWh}$
Total Process Energy Consumed	$4 + 16 = 20 \text{ MWh}$
Energy supplied during hour 1	$(4 \text{ M} / 0.8)(1 \text{ hr}) = 5 \text{ MWh}$
Energy supplied during hour 2 and 3	$(8 \text{ MW} / 0.8)(2 \text{ hr}) = (10 \text{ MW})(2 \text{ hr}) = 20 \text{ MWh}$
Total Energy Supplied	$5 + 20 = 25 \text{ MWh}$
Average Energy Efficiency	$20 / 25 = 80\%$

From reviewing the table, it is clear that the biggest energy losses from the process occurred during hours 2 and 3. If the end user selecting the equipment or the equipment designer could improve the efficiency at a compromise elsewhere, it would be better to have a higher efficiency during the portion of the process that more power is used for longer periods of time. Assume there was another piece of equipment that could be used to control the process that had a maximum efficiency of 90% when supplying the load power of 8 MW and only 70% when supplying the load power of 4 MW. Table 2.2 shows the updated energy calculations.

Table 2.2: Net energy consumed for a more optimized design

Energy consumed by load during hour 1	4 MWh
Energy consumed by load during hour 2 and 3	16 MWh
Total Process Energy Consumed	20 MWh
Energy supplied during hour 1	$(4\text{M}/0.7)(1\text{hr}) = 5.71 \text{ MWh}$
Energy supplied during hour 2 and 3	$(8\text{MW}/0.9)(2\text{hr}) = 17.78 \text{ MWh}$
Total Energy Supplied	$5.71 + 17.78 = 23.49 \text{ MWh}$
Average Energy Efficiency	$20/23.49 = 85\%$

As can be seen from comparison of Table 2.1 and Table 2.2, the energy usage for the second design is 23.49 MWh rather than the 25 MWh for the first design. The average energy efficiency for controlling the process was shown to increase from 80% to 85%. What if the user had a range of possible equipment designs or possible design compromises, what would be the ideal selection for reduced energy usage? If calculations as performed in Table 2.1 and Table 2.2 were performed for all possible combinations, the system that uses the least energy for the process or has the highest

average efficiency would be the ideal choice. Since the computations are tedious, a system designer may use their understanding of how efficiency varies based on the design constraints to develop a math model of efficiency as a function of the design constraints. If load power vs. time characteristics were also known, they could be included in a math equation of power as a function of time. A computer algorithm could then be written to perform the computations identified in the above tables and iteratively change system design constraints while keeping track of the average efficiency for each possible combination. The system with the maximum average efficiency would utilize the least energy when controlling the process, and would correspondingly cost the end user less on their utility bill.

2.2 Simplified example applied using power factor

Similar to efficiency, power quality parameters such as *power factor* and harmonic distortion can be optimized for a process. Reduced *power factor* creates a number of problems as has been discussed and results in similar costs to large power consumers as does reduced energy efficiency. The simplified examples described for energy efficiency will now be extended to *power factor*. Assume the same 3 hour industrial process with the same load characteristics of Figure 2.2 is now supplied by electrical equipment that has very high energy efficiency but reduced *power factor*. The system is shown below in Figure 2.3.

Similar to the energy efficiency example, assume the design has a maximum *power factor* of 0.8 which applies for the range of load conditions. Table 2.3 identifies the reactive power requirements computed from equation (2.1) [19].

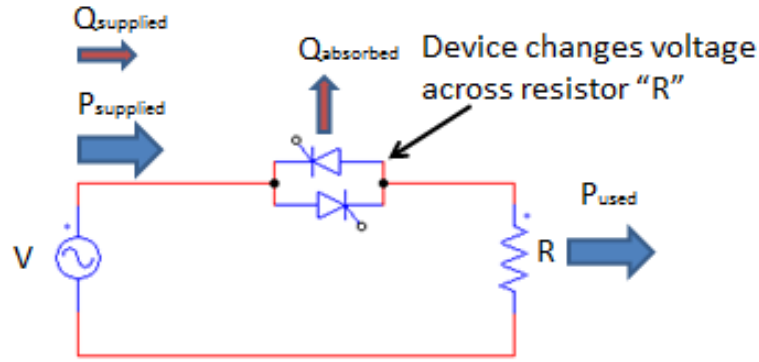


Figure 2.3: Power and reactive power delivery

$$Q = \sqrt{(P / pf)^2 - P^2} \tag{2.1}$$

Table 2.3: Real and reactive power required by the process load

	Real Power (P)	Reactive Power (Q)
Hour 1	4 MW	3 MVAR
Hour 2 and 3	8 MW	6 MVAR

Table 2.4 computes the time average real power for the process and time average reactive power and then a time average computation for apparent power \$S\$ is performed and a calculation for the average *power factor*. The following equations are used.

$$P_{avg} = (P_1 \cdot \Delta t_1 + P_2 \cdot \Delta t_2 + \dots + P_n \cdot \Delta t_n) / t \tag{2.2}$$

$$Q_{avg} = (Q_1 \cdot \Delta t_1 + Q_2 \cdot \Delta t_2 + \dots + Q_n \cdot \Delta t_n) / t \quad (2.3)$$

$$pf_{avg} = \frac{P_{avg}}{\sqrt{P_{avg}^2 + Q_{avg}^2}} \quad (2.4)$$

$$t = \sum_{i=1}^n t_i \quad (2.5)$$

The average *power factor* can be seen to match the constant *power factor* of 0.8 as should be expected since it was applied throughout.

Table 2.4: Time weighted real, reactive and apparent powers

Time weighted average of P	$[(4\text{MW})(1\text{hr}) + (8\text{MW})(2\text{hr})]/3\text{hr} = 6.67 \text{ MW}$
Time weighted average of Q	$[(3\text{MVAR})(1\text{hr}) + (6\text{MVAR})(2\text{hr})]/3\text{hr} = 5 \text{ MVAR}$
Time weighted average of S	$(6.67^2 + 5^2)^{0.5} = 8.33 \text{ MVA}$
Average Power Factor	$6.67 / 8.33 = 0.8 \text{ or } 80\%$

Using a similar design compromise to that used for changing efficiency, a *power factor* of 0.7 is used during the first hour and a *power factor* of 0.9 is used during the second and third hours. The reactive power requirements are again computed and shown in Table 2.5 below. The time weighted average real, reactive and apparent powers and corresponding average *power factor* are shown in Table 2.6.

Table 2.5: Real and reactive power for optimized design

	Real Power (P)	Reactive Power (Q)
Hour 1	4 MW	4.08 MVAR
Hour 2 and 3	8 MW	3.87 MVAR

Table 2.6: Time weighted average of real, reactive and apparent power

Time weighted average of P	$[(4\text{MW})(1\text{hr}) + (8\text{MW})(2\text{hr})]/3\text{hr} = 6.67 \text{ MW}$
Time weighted average of Q	$[(4.08\text{MVAR})(1\text{hr}) + (3.87\text{MVAR})(2\text{hr})]/3\text{hr} = 3.94 \text{ MVAR}$
Time weighted average of S	$(6.67^2 + 3.94^2)^{0.5} = 7.75 \text{ MVA}$
Average Power Factor	$6.67/ 7.75 = 0.86 \text{ or } 86\%$

It can be seen from Table 2.6 that the average *power factor* is improved for the second design and the average apparent power supplied is lower. Similar to improving average energy efficiency, *power factor* can be improved for process conditions or load cycles that are repetitive or approximately repetitive. As with efficiency, a math model can be developed for the *power factor* as a function of the system design constraints. A math model can also be developed to show how the process conditions such as power vary over time. A computer algorithm could then be written to perform the logical iterations identified in the above tables and equations. The design constraints that provide the maximum average *power factor* would be ideal. Although the approach can be applied generally speaking to any system, a design using multiple transformer secondary taps and power electronic devices as was shown in Figure 2.3 will be analyzed for an industrial process in the next section and a computer algorithm approach will be applied to determine the optimal tap spacing for maximum average

power factor. The process for optimization of a desired variable, the objective function, through applied math and application of a computer algorithm is commonly performed for engineering systems but is not traditionally performed for power factor and electrical energy efficiency for process industries [23, 24].

2.3 Power factor improvement method applied to a repetitive industrial process

Consider the following batch (repetitive) industrial process using electrical heating where a high power and a correspondingly high voltage is used at the beginning of the process. Later in the process a substantial reduction in load power is required and the voltage is correspondingly reduced. The lower power portion of the process is operated at that power level for less time than the higher power region similar to the examples discussed in section 2.1. The particular process characteristics could be any level of complexity.

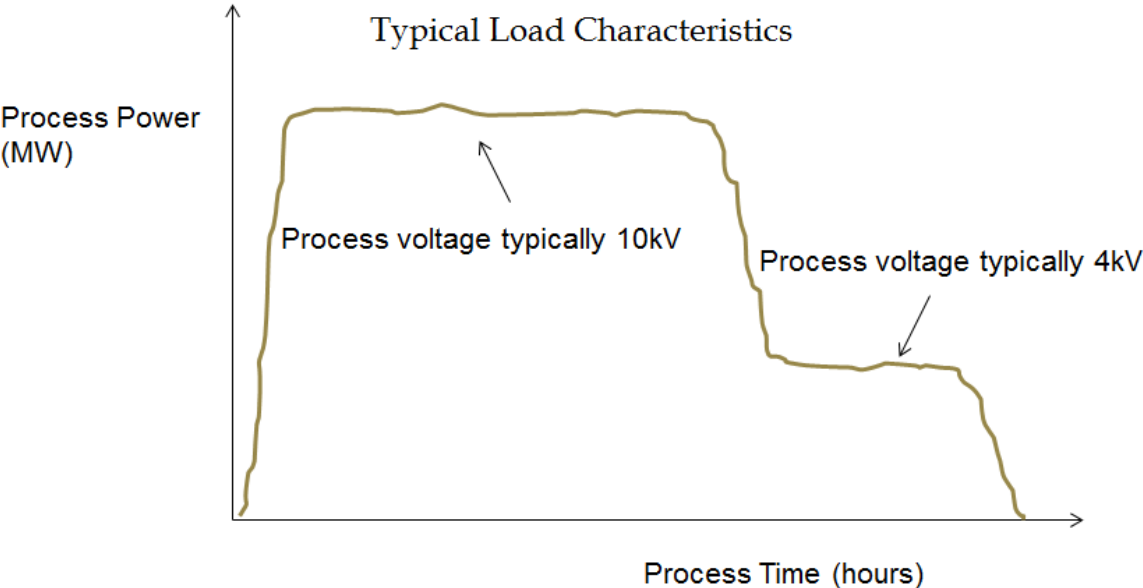


Figure 2.4: Example of an industrial process utilizing electrical heating

The above process will initially be analyzed utilizing two unique transformer design configurations, both using three secondary voltage taps as is shown in Figure 2.5. It will be assumed that the above voltage tap should remain at the nominal 13.8kV and only the bottom two taps may be adjusted. The first transformer referred to as *Transformer Design 1* is designed to ensure the minimum *power factor* is the same for all regions between the bottom voltage tap and the upper voltage tap at 13.8kV. The second, *Transformer Design 2* is designed to have a higher minimum *power factor* in the region using more power for longer periods of time and lower minimum *power factor* for the second region of the process. The *power factor* plots for design 1 and 2 are shown in Figure 2.6 and Figure 2.7 respectively.

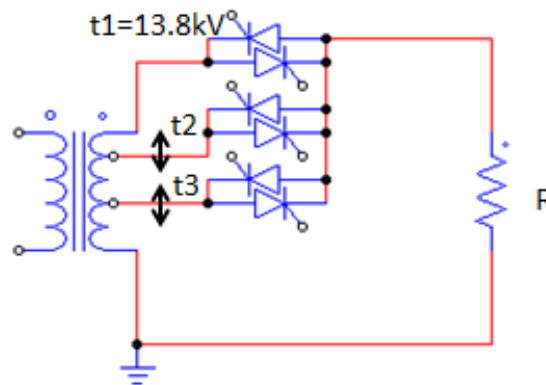


Figure 2.5: Transformer utilized for resistive heating process control

The transformer designs will be analyzed by applying the methodology outlined in section 2.1, however, a computer algorithm will be applied to perform the computations. The *power factor* for each design is a function of the output voltage and transformer tap spacing, and the middle tap is at 5.3kV and 8kV for design 1 and 2 respectively. In order to determine the reactive powers and compute the average *power*

factor for the process, the process voltage and power must be known as a function of time. The plot in Figure 2.8 shows an example of the required process information. The power and voltage could take on any complex nature as determined by the process.

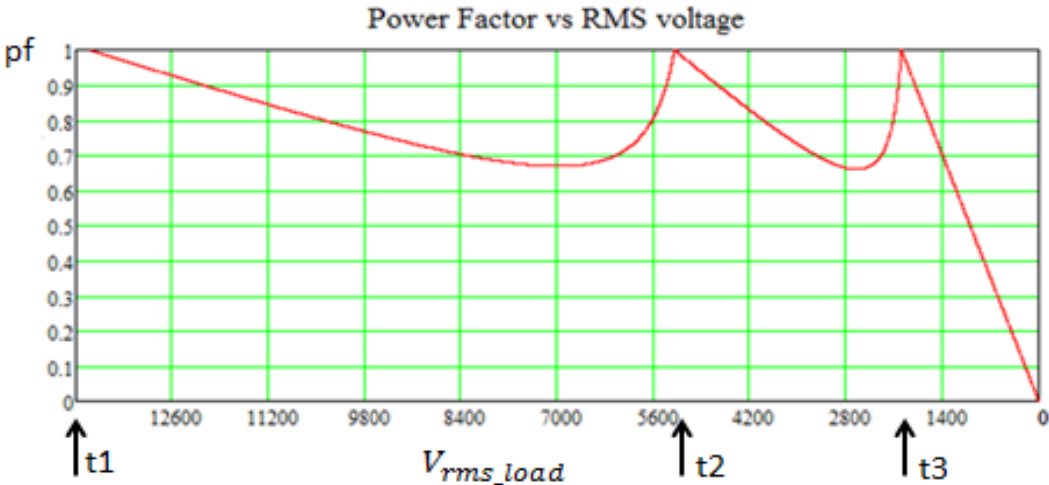


Figure 2.6: Transformer Design 1

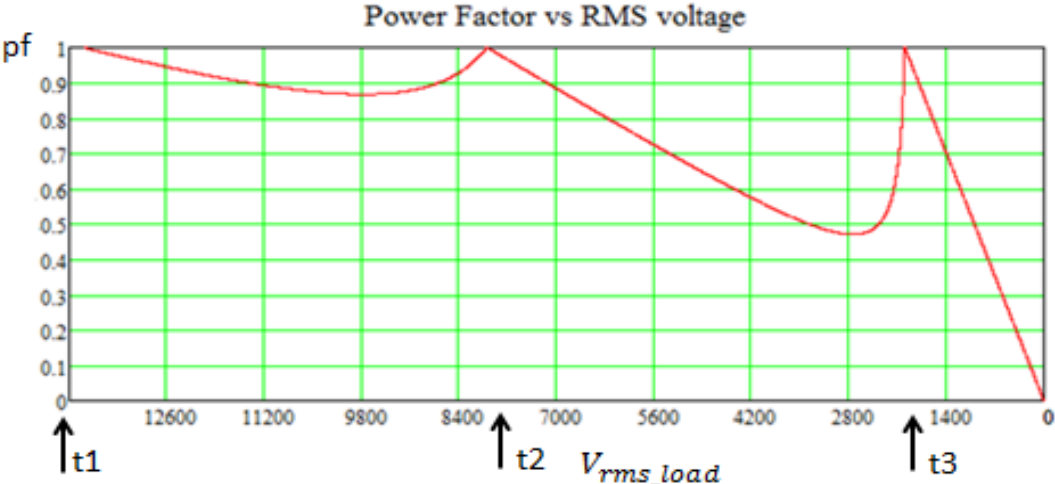


Figure 2.7: Transformer Design 2

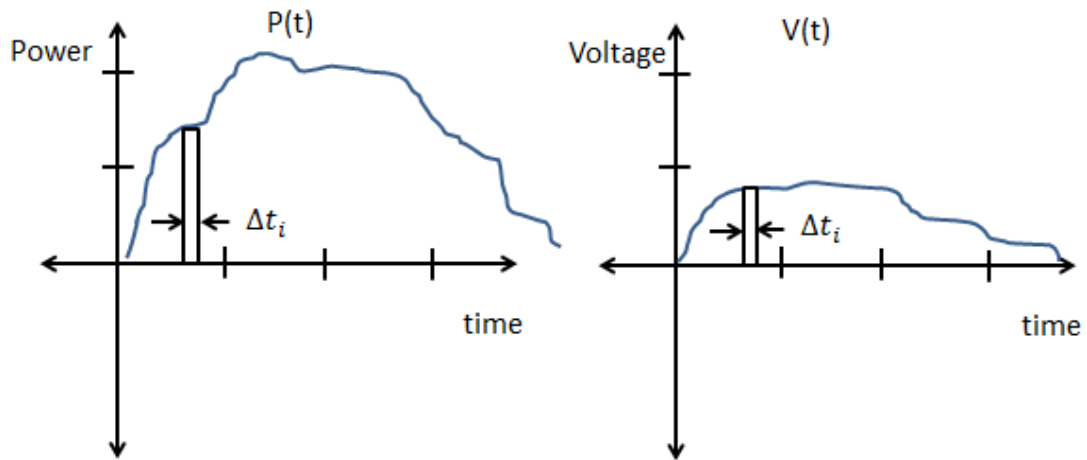


Figure 2.8: Required process information

For determining the ideal voltage tap spacing for the transformer design shown in Figure 2.5, the computer algorithm steps are outlined in the algorithm flow chart shown in Figure 2.9.

A summary of the required information for optimization are included in the bulleted list below:

- Objective function for optimization = *power factor*
- Required Process Information
 - a. Voltage(time)
 - b. Power(time)
- Develop a math model as follows:
 - a. *power factor*(voltage, tap spacing)

- Choose an appropriate time interval Δt_i where process conditions are approximately constant (i.e. 15 minutes)

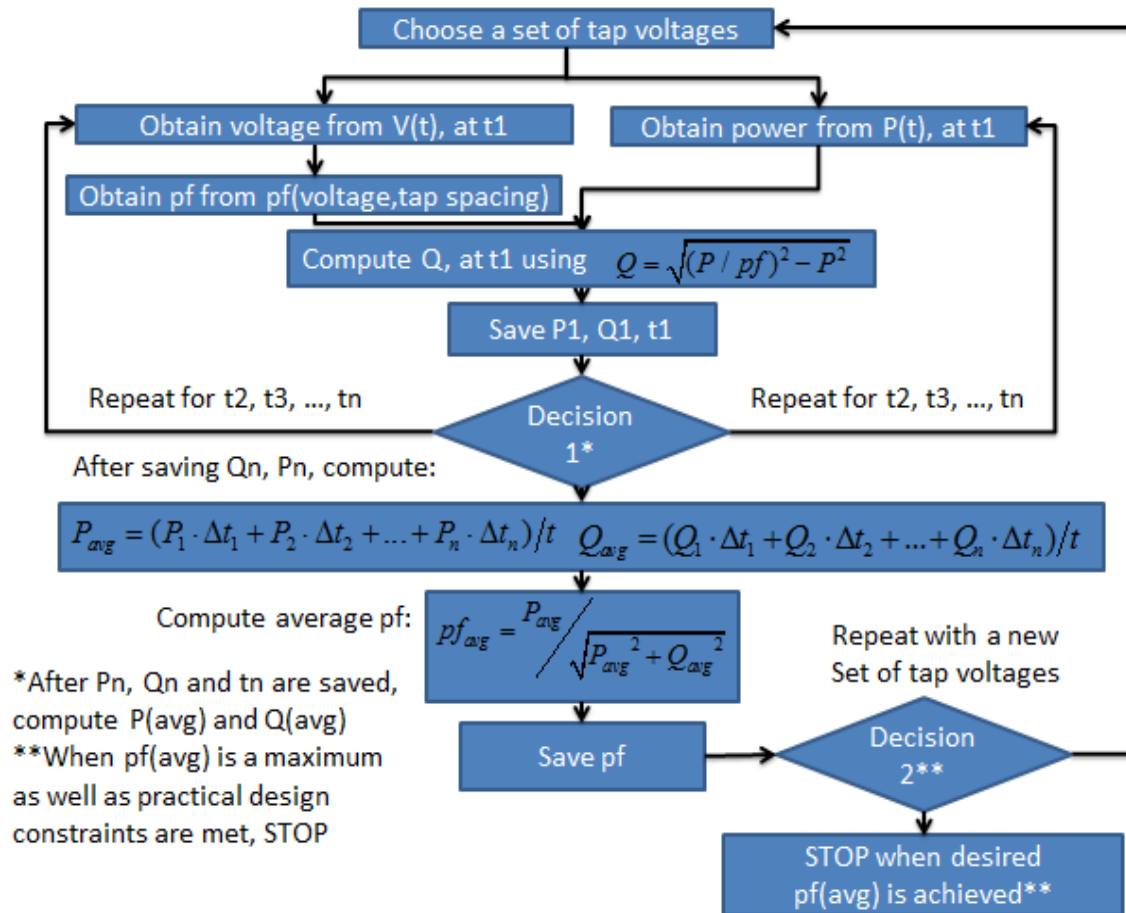


Figure 2.9: Algorithm flow chart

Before optimizing the transformer tap spacing to determine the maximum average *power factor*, a simple example for voltage and power vs. time will be applied to test that the algorithm predicts changes in average *power factor* according to the logic previously outlined in section 2.1 (according to time and power weighting).

The first test example is for a 40 hour process. The power is set to a value of 100 kW for the first 30 hours and a value of 20 kW for the last 10 hours. The corresponding voltages are 10kV and 4kV for the two process regions respectively. The power and voltage vs. time are shown below in Figure 2.10.

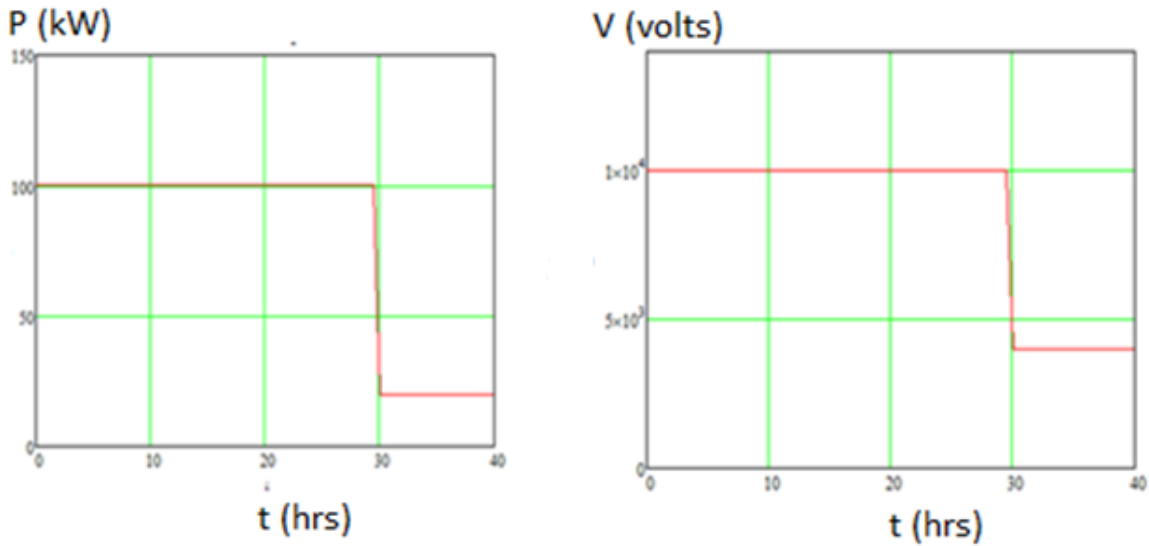


Figure 2.10: Process example 1 power and voltage requirements

The average *power factor* is computed for the two different transformer designs and is shown below in Table 2.7.

Table 2.7: Algorithm results for different center tap configurations

Transformer Design 1	Transformer Design 2
Voltage taps: 13.8kV, 5.3kV, 2kV	Voltage taps: 13.8kV, 8kV, 2kV
Average displacement factor = 0.89	Average displacement factor = 0.93

As to be expected from intuition, the *Transformer Design 2* with a higher *power factor* for the region using more power for a longer period of time has a higher average *power factor* of 0.93 compared to 0.89 of *Transformer Design 1*.

The next test is to see the effect of reducing the time the process spends in the higher power region and increase the time in the lower power region to an even split (20 hours each). The corresponding power and voltage characteristics are shown below in Figure 2.11.

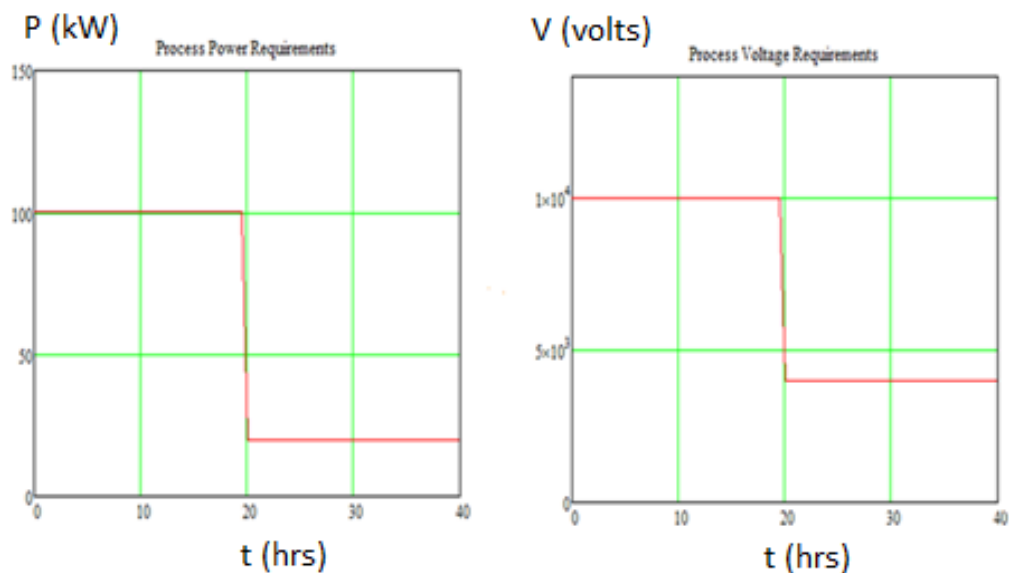


Figure 2.11: Process example 2 power and voltage requirements

In the above example, it would be expected to have less of a relative difference in *power factor* between the two tap regions since there is less time weighting of the higher power region. The results computed are shown below in Table 2.8. The average *power factor* for *Transformer Design 2* dropped from 0.93 to 0.91. *Transformer Design 1* *power factor* increased slightly from 0.89 to 0.891.

Table 2.8: Algorithm results for different center tap configurations

Transformer Design 1	Transformer Design 2
Voltage taps: 13.8kV, 5.3kV, 2kV	Voltage taps: 13.8kV, 8kV, 2kV
Average displacement factor = 0.891	Average displacement factor = 0.91

Now that the algorithm has been confirmed to behave as expected, it will be applied to similar but more complex process where the power and voltage both vary continuously to show the advantage of applying a computer algorithm approach to optimizing the transformer tap spacing. The process still has an obvious region of higher power usage and that of lower usage, however, the continuous variation adds an element of complexity. The process conditions are shown below in Figure 2.12.

Transformer Design 1 and *Transformer Design 2* will both be analyzed and compared. Additionally, a third design, *Transformer Design 3*, where the algorithm was applied to determine optimum transformer tap spacing to achieve the highest maximum average *power factor* is compared. The plot of *power factor* for the third design is shown in Figure 2.13 and can be seen to be similar to design 2 but with the bottom voltage taps increased slightly (8kV to 10.8kV and 2kV to 2.3kV respectively).

Table 2.9 shows the average *power factor* computations for the three designs. *Transformer Design 2* still had an improved *power factor* over that of *Transformer Design 1*, 0.938 compared to 0.903. *Transformer Design 3* has the highest average *power factor*, 0.971.

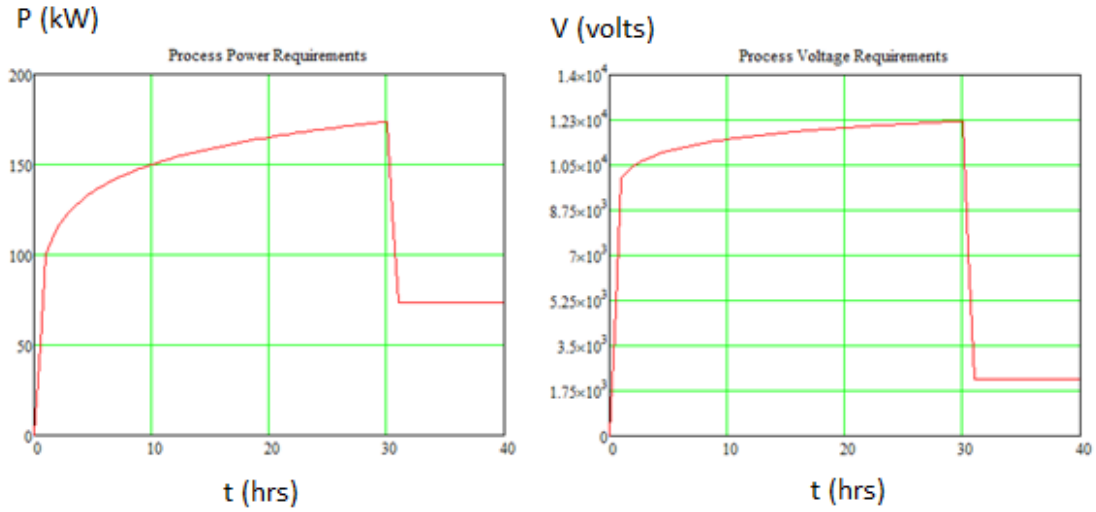


Figure 2.12: Process with continuously varying conditions

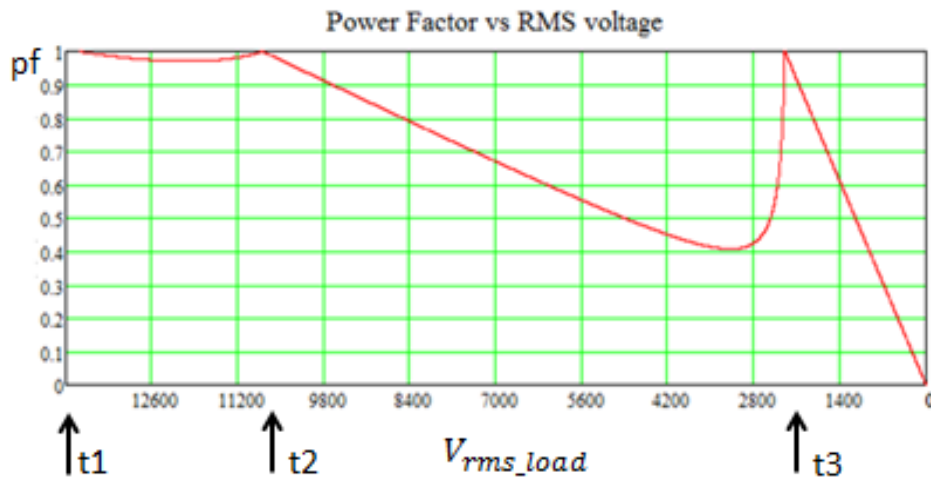


Figure 2.13: Transformer Design 3

When comparing the transformer *power factor* graph for design 3 to that of 2 (Figure 2.12 and Figure 2.13), the benefit of the algorithm can be seen as it is not obvious what an ideal compromise should be. For more complex processes and when more voltage taps may be used, the algorithm provides the greatest benefit.

Additionally, other aspects of the design can be evaluated and compared such as the potential benefit of including an additional transformer tap.

Table 2.9: Transformer design 1, 2 and 3 average power factor

Transformer Design 1	Transformer Design 2	Transformer Design 3
Voltage taps: 13.8 kV, 5.3 kV, 2 kV	Voltage taps: 13.8 kV, 8 kV, 2 Kv	Voltage taps: 13.8kV, 10.8 kV, 2.3 kV
Average power factor = 0.903	Average power factor = 0.938	Average power factor = 0.971

In a typical processing plant, many loads are likely to be supplied. An example is shown in Figure 2.14 where 8 systems are supplied from the same bus. The more systems supplied that have been optimized, the net *power factor* of all systems will tend to approach the average value for a single system (i.e. each individual system may be at different operating points). For transformer tap spacing algorithm, the *displacement power factor* was chosen as the variable for improvement, despite having a reduced *distortion factor* contribution to *power factor*. For many systems operating on a bus, harmonic current cancellations may occur and can be significant, reducing the THD₁ for the bus and the *distortion factor* may become negligible. For example a THD₁ of 10% results in a *distortion factor* of 0.995, small compared to the *displacement factor* which does not cancel for additional systems. Appendix C specifically investigates harmonic cancellation in more detail.

A final note is that that many processes do not have conditions that repeat exactly but may have a consistent nature as to how they are controlled. Analyzing a

large volume of statistical data for a system can be used to provide better information relative to how the system typically behaves [25, 26].

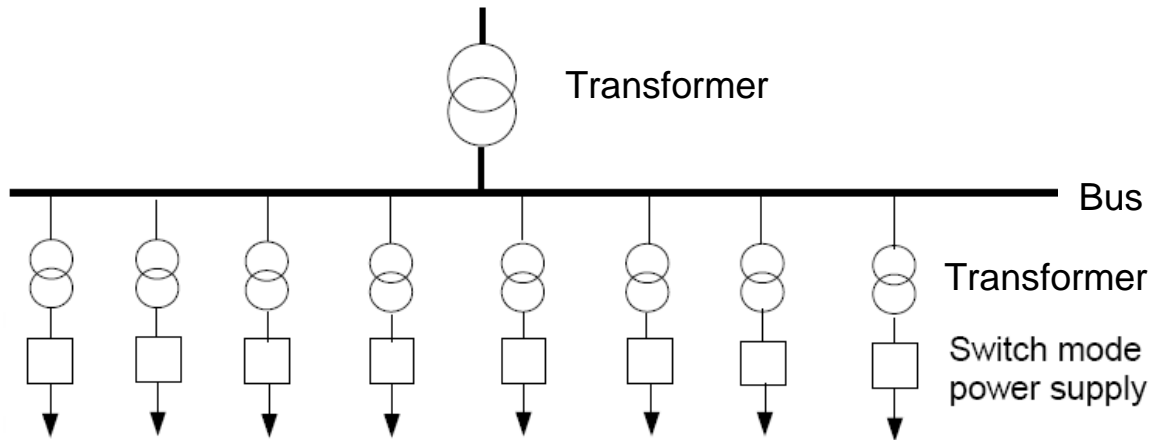


Figure 2.14: Industrial bus with 8 systems

2.4 Design optimization summary

As outlined in section 2.1 and 2.2, processes or load cycles with variable conditions that repeat over time (i.e. voltage and power) can further be improved for maximizing *power factor* (or energy efficiency) during the design process. A math model must be developed for *power factor* as a function of system design constraints (i.e. transformer taps voltages and load voltage). If process conditions are known for how power and voltage change with time, a computer algorithm can be written to perform computations to maximize average *power factor*. Applying an algorithm approach to improving design provides the proper weighting of variables and can result in substantial improvement in average *power factor* for complex load characteristics. If the average *power factor* is improved for a single system, a plant operating with many systems will have an improved *power factor* and the more systems operating in the

plant, the *power factor* will approach the average value computed for a single system. Additionally, the more systems operating in the plant, the plant deviations from the average value of the single system will be smaller. Since many processes may not repeat exactly, analyzing statistical data can be used to provide information relative to how the system typically varies.

CHAPTER 3 – ECONOMIC EVALUATION

As identified in reference [3], a recent charge (year 2012) from Xcel Energy, a public service company of Colorado, is \$0.109/(kWh) for a residential customer. It should be noted that the \$0.109/(kWh) rate will vary for each state, however.

Additionally, industrial consumers are often charged at a lower rate than residential customers due to contracts for purchasing large amounts of energy over time [6]. For simplicity, a round number of \$0.10/(kWh) will be used as the energy charge for all examples identified below.

In addition to the energy charges, as was discussed in chapter 1, utilities typically charge large industrial consumers for reduced *power factor*. There are a range of different types of fee schedules for how power factor is charged. An example of a fee structure is shown in Table 3.1 [6]. The example shown in the table shows a 1% additional charge is applied to the customer for every 1% drop in *power factor* below 0.95. If the *power factor* was 0.85, the customer would be charged $(1.10)(\text{energy bill})$. If the customer were charged based on kVAh for $\text{pf} < 0.95$, the charge would be $(\text{energy bill}) + (\text{energy bill})(1/0.85 - 1/0.95) = (1.12)(\text{energy bill})$, as can be seen, the charges are comparable (2% difference). There are many possible ways that the utility can charge for *power factor* but generally speaking, they are on par with charges per kVAh. For the design examples of chapter 2 for improving transformer design 1, 2 and 3, the *power factor* was improved greater than 0.95 for design 3. Additionally, the *power factor* for each design were not 0.1 deviations from 0.95. To get a sense of the relative potential cost savings, it will be assumed that *power factor* is charged based on kVAh.

Table 3.1: Example power factor fee schedule

Energy usage charge	Plant power factor	Additional Charge
(\$0.10/kWh)(# kWh used)	Pf between 1-0.95	No additional charge
(\$0.10/ kWh)(# kWh used)	Pf between 0.94-0.95	1% of energy usage
(\$0.10/ kWh)(# kWh used)	Pf between 0.93-0.94	2% of energy usage
(\$0.10/ kWh)(# kWh used)	Pf between 0.92-0.93	3% of energy usage
(\$0.10/ kWh)(# kWh used)	Pf between < 0.92	Additional 1% charge for each 0.1 drop in pf

Assume the industrial plant has an average of 20 MW of loads that are operating throughout the year that have reduced *power factor*. The above number is a reasonable number for a large processing plant and the total connected load could be much higher depending on the size of the plant and the type of process [17]. The numbers chosen are only to get a sense of potential cost savings, however, the detailed economics must be applied to the specific situation being evaluated. The plant energy costs are computed from the below equations.

$$\text{Energy} = (P)(t) \tag{3.1}$$

$$\text{Energy Costs} = (\text{Energy})(\text{rate}) \tag{3.2}$$

For the example provided, the total energy cost is as follows (it should also be noted that the number is reasonable for a large process plant and could be much higher [17]):

$$\text{Energy Cost} = (20,000 \text{ kW})(8760 \text{ h/year})(\$0.10/(\text{ kWh})) = \$17.5 \text{ million/year}$$

The 3 transformer designs identified in Chapter 3 will be compared to get a sense for the potential annual savings. It is important to note, however, that the design examples analyzed were only to show the advantage of an algorithm approach and much more complex processes may have a much higher improvement [17]. The *power factor* for the three designs is shown below in Table 3.2 for comparison.

Table 3.2: Transformer designs for economic comparison

Transformer Design 1	Transformer Design 2	Transformer Design 3
Voltage taps: 13.8 kV, 5.3 kV, 2 kV	Voltage taps: 13.8 kV, 8 kV, 2 kV	Voltage taps: 13.8kV, 10.8 kV, 2.3 kV
Average power factor = 0.903	Average power factor = 0.938	Average power factor = 0.971

For charges directly based on kVAh, the annual utility bill is computed as follows:

$$\text{Annual Savings} = (\text{Energy charges})(1/\text{pf}_{\text{initial}} - 1/\text{pf}_{\text{improved}})$$

The annual savings is applied to the 3 transformer designs as follows:

1) *Transformer Design 2* to that of *Transformer Design 1*

The *power factor* was improved from 0.903-0.938. The savings would be as follows:

$$\text{Annual Savings} = (\$17.5 \text{ million/year})(1/0.903 - 1/0.938) = \mathbf{\$723,000/year}$$

2) *Transformer Design 3* to that of *Transformer Design 2* the *power factor* was improved from 0.938-0.971. The savings would be as follows:

$$\text{Annual Savings} = (\$17.5 \text{ million/year})(1/0.938 - 1/0.971) = \mathbf{\$634,000/\text{year}}.$$

3) *Transformer Design 3* to that of *Transformer Design 1* the *power factor* was improved from 0.903-0.971. The savings would be as follows:

$$\text{Annual Savings} = (\$17.5 \text{ million/year})(1/0.903 - 1/0.971) = \mathbf{\$1.36 \text{ million/year}}.$$

The above examples help provide an idea of potential savings for a small improvement in *power factor*. It must be considered, however, that more complex processes can have even more substantial improvement than the examples discussed. The improvement may be the difference between the customer being charged a hefty fee or not. Regardless of the fee schedule that is applied, any improvement in *power factor* will reduce transmission losses, improve voltage regulation and reduce equipment sizing, all of which does cost the utility more and there are no guarantees that *power factor* fee schedules will remain fixed at where they are today. In addition to optimizing designs for improved *power factor* during the design stage, return on investment (ROI) calculations should be performed on older equipment designs to assess the potential savings for replacing equipment. See reference [27] for detailed economic evaluation considerations. Additionally, variability in how equipment may be utilized and other unknowns should be considered when performing economic evaluations or when making business decisions [25, 26].

CHAPTER 4 – SUMMARY AND CONCLUSIONS

Electrical power systems are used to convert and transport energy over long distances where it can be reconverted in the form of mechanical energy (via electric motors) or heat (via electric heaters) or other possible forms for the end user at locations remote from the source. The electrical power system has the advantage of being able to transport energy over large distances relatively efficiently. The term *power* is used more frequently, however, it is important to understand that *power* is the rate of energy usage (energy/time). An example of a ton of coal was utilized to represent a given amount of energy and higher power usage will dictate how quickly that ton of coal is used up.

The purpose of the electrical generation, transmission and distribution system is to transport energy so that it can be used by the end user (industrial, commercial or residential). Although the end user primarily charged for the energy they consume (kWh), they indirectly pay for other costs such as capital costs of equipment, labor, etc. The way the end user uses the power supplied to them can create additional complications and costs for the electrical utility and those complications are generally captured with the term *power quality*. Although there are a number issues under the umbrella term *power quality*, two specific related *power quality* terms, *power factor* and *total harmonic distortion* were defined and their negative effects discussed. Improving *power quality* such as improved *power factor* and *total harmonic distortion* has the following benefits:

- 1) Improve energy transmission efficiency by reducing system losses
- 2) Improve voltage regulation
- 3) Free system capacity
- 4) Improved system security
- 5) Decrease costs by reducing equipment size
- 6) Improved interchange transfer capability
- 7) Improved system operation
- 8) Increase the life of plant equipment
 - a. Reduce heat loading which degrades insulation life of plant equipment
 - i. Reduced *power factor* increases line currents increasing equipment size and increases transmission $(I^2)R$ losses
 - ii. Harmonic currents increase $(I^2)R$ losses through skin effect heating and additionally increase transformer core losses. Eddy current losses are proportional to frequency²
 - b. Voltage distortion within the plant associated with harmonic currents creating voltage drops across system impedances which are subtracted from the originally sinusoidal supply voltage can create problems for other plant connected equipment such as motors.

Reduced *power factor* is such a common problem created by the loads utilized by large industrial consumers that electrical utilities typically charge based on reduced *power factor*. Traditional methods for improving *power factor* were discussed such as using *power factor* correction capacitors or including additional transformer taps for power electronic devices providing process control. For processes or load cycles that

have a repetitive nature, further improvement in *power factor* can be made during the design process. A technique of mathematically modeling the system and writing a computer algorithm to determine the design compromises that result in the highest average *power factor* was discussed. Specifically, a transformer with 3 secondary taps was investigated with the computer algorithm approach to determine the optimum nominal voltage tap spacing. For processes with complex characteristics where the tradeoffs may not be obvious, the algorithm approach to improving design has the greatest benefit and can provide substantial improvement.

The final section provided examples of the economic impacts of reduced *power factor* and how a small improvement through the discussed optimization techniques can result in substantial annual savings for the end user. Although design optimization is best suited in the planning stages, the economics and return on investment for replacing equipment should be considered by the end user.

4.1 Future Work

Other potential applications for optimization type work include transmission system design, electric motors for process industries, integrated smart grid applications, etc. For the electric utility, the load cycles are the residential, commercial and industrial customers. Known information about how those load cycles typically vary can be utilized to apply similar techniques to those that were outlined in this document.

REFERENCES CITED

- [1] "U.S. Energy Information Administration," [Online]. Available: www.eia.gov. [Accessed 5 November 2012].
- [2] C. C. f. E. Information, "What is electricity transmission?," [Online]. Available: <http://www.centreforenergy.com/AboutEnergy/Electricity/Transmission/Overview>. [Accessed 5 October 2012].
- [3] X. Energy, *private communication*, 2012.
- [4] J. R. Cogdell, *Foundations of Electric Circuits*, Upper Saddle River: Prentice Hall, Inc., 1999.
- [5] R. Dugan, M. McGranaghan, S. Santoso and H. and Beaty, *Electrical Power Systems Quality*, Mexico: McGraw-Hill, 2003.
- [6] E. C. I. Continental Divide, "Large Industrial Transmission Service," [Online]. Available: <http://www.cdec.coop/content/large-industrial-transmission-service>. [Accessed 20 October 2012].
- [7] J. Faiz and B. Siahkollah, "New Solid-State Onload Tap-Changers Topology for Distribution Transformers," *Power Delivery, IEEE Transactions on*, vol. 18, no. 1, pp. 136-141, 2003.
- [8] S. J. Chapman, "Introduction to Power Electronics", *Electric Machinery Fundamentals*, 3rd edition, New York: McGraw-Hill, 1999.
- [9] A. M. Trzynadlowski, *Introduction to Modern Power Electronics*, second edition, Hoboken: John Wiley & Sons, 2010.
- [10] K. J., S. M. and V. G., *Principles of Power Electronics*, Addison-Wesley, 1991.
- [11] S. Mohagheghi, *EGGN 580: Electric Power Quality, Fourier Series*, Golden: Colorado School of Mines, 2012.
- [12] E. A., "Powers in Nonsinusoidal Situations - A Review of Definitions and Physical Meaning," *Power Delivery, IEEE Transactions on*, vol. 5, no. 3, pp. 1377-1389, 1990.
- [13] P. Sen, *EGGN 584: Power Distribution Systems Engineering*, Golden: Colorado School of Mines, 2011.
- [14] G. R., "Harmonic Distortion of the Mains Voltage by Switched-Mode Power Supplies - Assessment of Future Development and Possible Mitigation," in *European Power Electronics Conference*, 1989.

- [15] P. K. Sen, *EGGN 583: Advanced Electrical Machine Dynamics*, Golden: Colorado School of Mines, 2012.
- [16] O. T.M. and C. K.R., "the effects of power system harmonics on power system equipment and loads," *Power Appar. Syst. IEEE Transactions on*, Vols. PAS-104, no. 9, pp. 2255-2263, 1985.
- [17] S. West and D. Rabosky, *private communication*, 2011.
- [18] P. Sen, "EGGN 389: Fundamentals of Electric Machinery," Colorado School of Mines, Golden, 2011.
- [19] J. D. Glover, M. S. Sarma and T. J. Overbye, *Power System Analysis*, 5th edition, Stamford: Cengage Learning, 2012, 2008.
- [20] R. Ammerman, *EGGN 487: Analysis and Design of Advanced Energy Systems*, Golden: Colorado School of Mines, 2012.
- [21] M. N., U. T. and R. W., *Power Electronics: Converters, Applications, and Design*, second edition, New York: John Wiley & Sons, 1995.
- [22] T. I. o. E. Engineers, *Recommended Practice for Establishing Transformer Capability when Supplying Nonsinusoidal Load Currents*, New York: ANSI/IEEE C57.110-1986, 1986.
- [23] B.-M. S., J.-C. C. J.-C., R. S., H. E., B. D., G. Z., A. M. and L. D., "Design of a Boost Power Factor Correction Converter Using Optimization Techniques," *Power Electronics, IEEE Transactions on*, vol. 19, no. 6, pp. 1388-1396, 2004.
- [24] A. Isfahani, E. B.M. and L. H., "Design Optimization of Low-Speed Single-Sided Linear Induction Motor for Improved Efficiency and Power Factor," *Magnetics, IEEE Transactions on*, vol. 44, no. 2, pp. 266-272, 2008.
- [25] M. Walls, *EBGN 560 - Decision Analysis*, Golden: Colorado School of Mines, 2012.
- [26] R. Clemen and T. Reilly, *Making Hard Decisions with Decision Tools*, Mason: Cengage Learning, 2001.
- [27] F. Stermole and J. Stermole, *Economic Analysis & Investment Decision Methods*, thirteenth edition, Lakewood: Investment Evaluations Corporation, 2012.
- [28] M. R. Lindeburg, *Engineer-In-Training Reference Manual*, 8th edition, Belmont: Professional Publications, Inc., 2002.
- [29] R. L. Burden and J. D. Faires, *Numerical Analysis*, seventh edition, Pacific Grove: Wadsworth Group. Brooks/Cole, 2001.

- [30] C. A., L. R. and P. A., "Estimation of net harmonic currents due to dispersed non-linear loads in residential areas," in *Harmonics and Quality of Power Proceedings, 8th International Conference*, 1998.
- [31] Y. Baghzouz, "Probabilistic Modeling of Power System Harmonics," *Industry Applications Society, IEEE Transactions on*, Vols. IA-23, no. 1, pp. 173-180, 1987.
- [32] Y. Hegazy and M. Salama, "Calculations of diversified harmonic currents in electric distributions systems," *Generation, Transmission and Distribution, IEEE Transactions on*, vol. 150, no. 6, pp. 651-658, 2003.
- [33] A. J., B. D. and B. P., *Power System Harmonics*, New York: John Wiley & Sons, 1985.

APPENDIX A – MATH MODEL DEVELOPMENT

To derive the relationships for *power factor* and RMS voltage and current on the primary and secondary for continuous operation between a lower and higher voltage tap, it will be considered that the primary voltage is a sine wave of peak amplitude “P” and no phase shift. The primary voltage can then be expressed in the following form $V_{\text{primary}} = P\sin(x)$. The RMS voltage of the primary is $V_{\text{rms_primary}} = P/\sqrt{2}$. The waveform is shown in Figure A-1 for half a cycle. The variable x is denoted by the natural unit of radians, however, the time relationships and angle in degrees can be converted by using equations (A-1), (A-2) and (A-3) [28].

$$x = \omega t, \tag{A-1}$$

where ω is the angular frequency in radians/second and t is in seconds

$$\omega = 2\pi/T, \tag{A-2}$$

where T is the period in seconds

$$\theta = x(180/\pi), \tag{A-3}$$

where θ is the angle in degrees

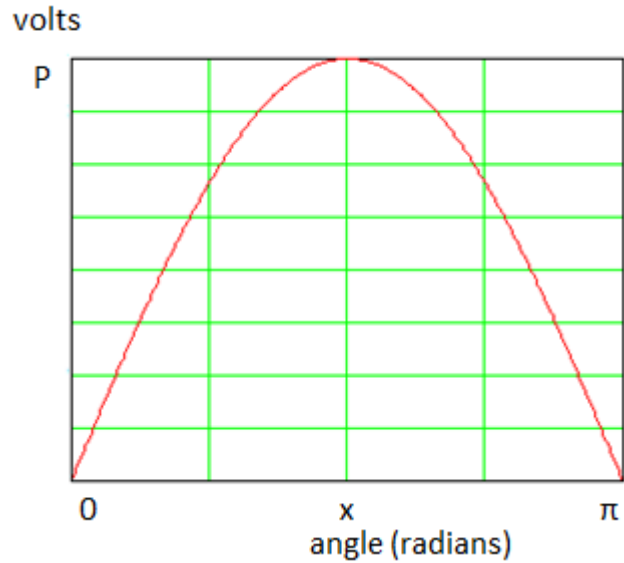


Figure A-1: Half a cycle for a primary voltage with peak amplitude “P”

It is next considered that there are a pair of voltage taps on the secondary of the transformer where one is of a lower voltage and is denoted by the nominal RMS value of t_{lower} and the second has a higher voltage with a nominal RMS value denoted by t_{upper} . The peak amplitudes for the voltage waveforms on the secondary are denoted by “A” for the lower voltage tap and “B” for the upper voltage tap and are related to the RMS tap voltages by equations (A-4) and (A-5). The circuit is shown below in Figure A-2 and an assumed load resistance of $R=1\Omega$ will be used for simplicity. When deriving the relationships for *power factor*, the load resistance R would cancel from the equations as will be identified during the derivations.

$$A = \sqrt{2}t_{\text{lower}} \tag{A-4}$$

$$B = \sqrt{2}t_{\text{upper}} \tag{A-5}$$

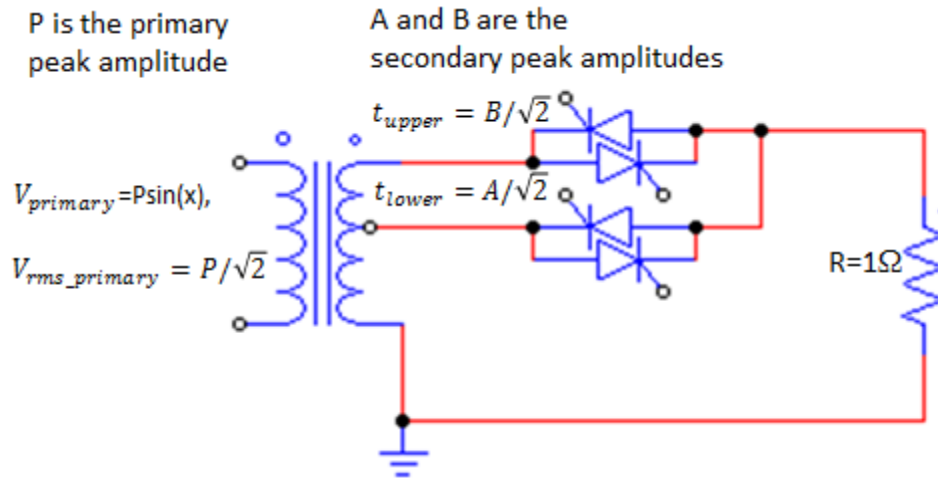


Figure A-2: Primary and secondary voltages with peak P, A and B respectively

To determine the RMS voltage on the transformer secondary (applied to the load) for any range of voltage from the lower voltage tap to the upper voltage tap, a firing angle ϕ will denote the switching from the lower voltage tap to the higher voltage tap. A firing angle of 180 degrees would indicate that the higher voltage tap voltage is never applied to the load and the load voltage would be $A \sin(x)$. A firing angle of 0 would indicate that only the upper tap voltage is applied to the load and the load voltage would be $B \sin(x)$. To determine the voltage for any angle between 0 and 180 degrees as is shown in Figure A-3, the definition of RMS voltage must be used [4]. Using the definition for RMS values, the transformer secondary voltage and current are shown in equations (A-6) and (A-7).

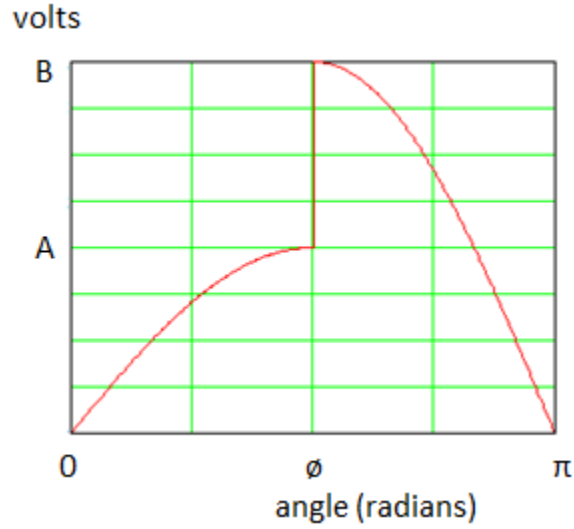


Figure A-3: Transformer secondary/load voltage

$$V_{rms_secondary}(\phi, A, B) = i_{rms_secondary}(\phi, A, B) = \frac{1}{\sqrt{\pi}} \sqrt{\int_0^{\phi} A^2 \sin^2 \theta d\theta + \int_{\phi}^{\pi} B^2 \sin^2 \theta d\theta} \quad (A-6)$$

$$V_{rms_secondary}(\phi, A, B) = \frac{1}{\sqrt{\pi}} \sqrt{\left(\frac{\phi}{2} - \frac{\sin(2\phi)}{4}\right) A^2 + \left(\frac{\pi}{2} - \frac{\phi}{2} + \frac{\sin(2\phi)}{4}\right) B^2} \quad (A-7)$$

The above equations are generically defined such that the voltage can be computed for any firing angle ϕ between a lower voltage tap $t_{lower} = A/\sqrt{2}$ and upper voltage tap $t_{upper} = B/\sqrt{2}$. If only a single upper voltage tap is used and t_{lower} is 0 volts, the resulting waveform is shown in Figure A-4 and is representative of the load voltage and current waveforms for a household light dimmer using phase angle control [8]. The RMS value for the secondary of a transformer for any number of voltage taps can be

determined and plotted by generically applying equation (A-7) between each lower and upper voltage tap.

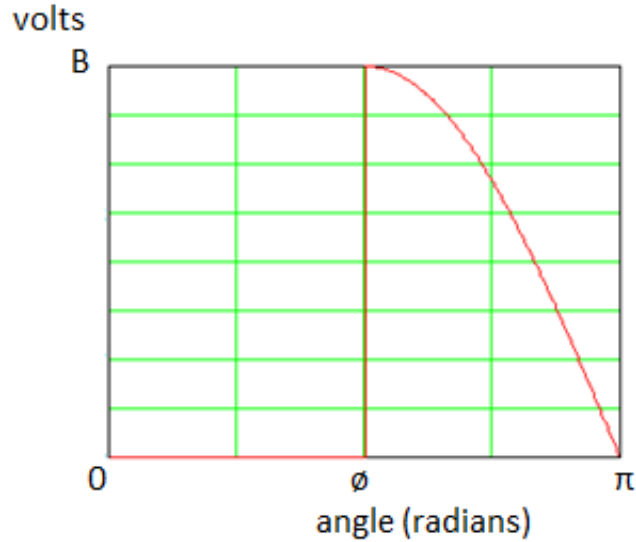


Figure A-4: Transformer secondary voltage with a lower tap of 0

Equation (A-7) expressed the RMS voltage across a load resistor of 1Ω between any pair of voltage taps was expressed as a function of their peak voltage amplitudes “A”, “B” and the firing angle ϕ . To determine the instantaneous voltage for any angle x in radians, the fourier coefficients must be determined and the resulting waveform expressed as a fourier series [5, 11] as is identified in equations (A-8), (A-9), and (A-10).

$$G1s(n, \phi, A, B) = \frac{2}{\pi} \left(0 + \int_0^{\phi} A \sin \theta \sin n\theta d\theta + \int_{\phi}^{\pi} B \sin \theta \sin n\theta d\theta + 0 \right) \quad (\text{A-8})$$

$$K1s(n, \phi, A, B) = \frac{2}{\pi} \left(0 + \int_0^{\phi} A \sin \theta \cos n\theta d\theta + \int_{\phi}^{\pi} B \sin \theta \cos n\theta d\theta + 0 \right) \quad (\text{A-9})$$

$$V_{secondary}(\phi, x, A, B) = \sum_{n=1}^{\infty} [G1s(2n-1)\sin[(2n-1)x] + K1s(2n-1)\cos[(2n-1)x]] \quad (A-10)$$

The secondary current for any load resistance “R” is expressed by (A-11).

$$i_{secondary} = V_{secondary}(\phi, x, A, B) / R \quad (A-11)$$

As was previously identified for simplicity in derivation of the *power factor* equations, a load resistance of $R=1\Omega$ was utilized such that $i_{secondary} = V_{secondary}$. The primary current, $i_{primary}$ can be related to the peak primary amplitude “P” and secondary peak amplitudes “A” and “B” by the corresponding transformer turns ratios [4]. The resulting primary current is shown in Figure A-5.

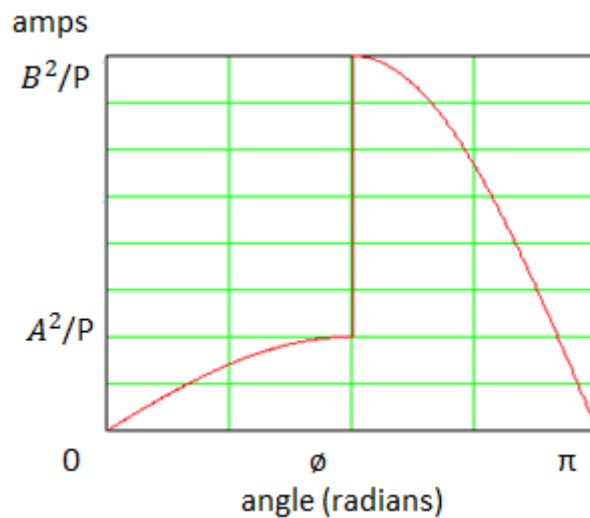


Figure A-5: Transformer primary current for a secondary load resistance of $R=1$

The value of the primary current for any angle x can be determined by expressing the primary waveform in terms of the fourier coefficients as was done for the secondary waveform [5, 11]. The fourier coefficients and primary current waveform are identified in equations (A-12), (A-13), and (A-14).

$$G1p(n, \phi, A, B) = \frac{2}{\pi} \left(0 + \int_0^{\phi} \frac{A \cdot A}{P} \sin \theta \sin n\theta d\theta + \int_{\phi}^{\pi} \frac{B \cdot B}{P} \sin \theta \sin n\theta d\theta + 0 \right) \quad (\text{A-12})$$

$$K1p(n, \phi, A, B) = \frac{2}{\pi} \left(0 + \int_0^{\phi} \frac{A \cdot A}{P} \sin \theta \cos n\theta d\theta + \int_{\phi}^{\pi} \frac{B \cdot B}{P} \sin \theta \cos n\theta d\theta + 0 \right) \quad (\text{A-13})$$

$$i_{primary}(\phi, x, A, B) = \sum_{n=1}^{\infty} [G1p(2n-1) \sin[(2n-1)x] + K1p(2n-1) \cos[(2n-1)x]] \quad (\text{A-14})$$

As was done for the secondary voltage and current, the RMS current of the primary current waveform shown in Figure A-5 is computed directly from the definition of an RMS quantity [4] and is shown in equation (A-15).

$$i_{rms_primary}(\phi, A, B) = \frac{1}{\sqrt{\pi}} \sqrt{\int_0^{\phi} \left(\frac{A \cdot A}{P}\right)^2 \sin^2 \theta d\theta + \int_{\phi}^{\pi} \left(\frac{B \cdot B}{P}\right)^2 \sin^2 \theta d\theta} \quad (\text{A-15})$$

To compute the *power factor*, equation (A-15) is simplified to the form shown in equation (A-16) and the primary RMS voltage expressed in terms of the peak amplitude “P” (A-17).

$$i_{rms_primary}(\phi, A, B) = \frac{1}{P\sqrt{\pi}} \sqrt{\int_0^{\phi} A^4 \sin^2 \theta d\theta + \int_{\phi}^{\pi} B^4 \sin^2 \theta d\theta} \quad (A-16)$$

$$V_{rms_primary} = \frac{P}{\sqrt{2}} \quad (A-17)$$

The *power factor* is related to the RMS quantities on the secondary and primary as is shown in equation (A-18). It should be noted that if a non-unity load resistance of “R” were included in the derivations, it would be present in both the secondary current and primary current equations and would cancel out when computing *power factor*.

$$pf(\phi, A, B) = \frac{(V_{rms_secondary}(\phi, A, B))(i_{rms_secondary}(\phi, A, B))}{(V_{rms_primary})(i_{rms_primary}(\phi, A, B))} \quad (A-18)$$

Substituting the previously defined equations, it can be shown that the peak amplitude “P” from the primary voltage cancels (equations (A-19) and (A-20)) when determining the *power factor*. The simplified formula for power factor is shown in equation (A-21) where it can be seen that the *power factor* does depend on the nominal secondary transformer tap spacing but is independent of the primary voltage.

$$pf(\phi, A, B) = \frac{\frac{1}{\pi} \left(\int_0^{\phi} A^2 \sin^2 \theta d\theta + \int_{\phi}^{\pi} B^2 \sin^2 \theta d\theta \right)}{\left(\frac{P}{\sqrt{2}} \right) \left[\frac{1}{P\sqrt{\pi}} \sqrt{\int_0^{\phi} A^4 \sin^2 \theta d\theta + \int_{\phi}^{\pi} B^4 \sin^2 \theta d\theta} \right]} \quad (A-19)$$

$$pf(\phi, A, B) = \frac{\frac{1}{\pi} \left(\int_0^{\phi} A^2 \sin^2 \theta d\theta + \int_{\phi}^{\pi} B^2 \sin^2 \theta d\theta \right)}{\frac{1}{\sqrt{2\pi}} \sqrt{\int_0^{\phi} A^4 \sin^2 \theta d\theta + \int_{\phi}^{\pi} B^4 \sin^2 \theta d\theta}} \quad (\text{A-20})$$

$$pf(\phi, A, B) = \sqrt{\frac{2}{\pi}} \left[\frac{\left(\frac{\phi}{2} - \frac{\sin(2\phi)}{4} \right) \left(\frac{A}{B} \right)^2 + \left(\frac{\pi}{2} - \frac{\phi}{2} + \frac{\sin(2\phi)}{4} \right)}{\sqrt{\left(\frac{\phi}{2} - \frac{\sin(2\phi)}{4} \right) \left(\frac{A}{B} \right)^4 + \left(\frac{\pi}{2} - \frac{\phi}{2} + \frac{\sin(2\phi)}{4} \right)}} \right] \quad (\text{A-21})$$

Equation (A-7) for the $V_{\text{rms_secondary}}$ was shown to only depend on the peak amplitudes A, B and firing angle ϕ . To express *power factor* as a function of $V_{\text{rms_secondary}}$ as denoted by equation (A-22), a computer program must be written to solve non-linear equation (A-7) for firing angle ϕ for a given $V_{\text{rms_secondary}}$. The *power factor* can then be determined from equation (A-21). See reference [29] for further details on solving non-linear systems of equations using iterative techniques.

$$pf(V_{\text{rms_secondary}}) \quad (\text{A-22})$$

Power factor can also be expressed in terms of the *displacement power factor* and *distortion factor*. The fourier coefficients must first be expressed in polar form as an amplitude and phase shift as is shown in equations (A-23) and (A-24) [11].

$$Ap(n, A, B, \phi) = \sqrt{G1p^2(2n-1) + K1p^2(2n-1)} \quad (\text{A-23})$$

$$\Phi p(n, A, B, \phi) = -1 \cdot a \tan \frac{K1p(2n-1)}{G1p(2n-1)} \quad (\text{A-24})$$

The transformer primary current is now expressed in the polar form as shown in equation (A-25).

$$i_{primary}(x, n, A, B, \phi) = \sum_{n=1}^{\infty} [Ap(n, A, B, \phi) \cdot \sin[(2n-1)x] + \Phi p(n, A, B, \phi)] \quad (\text{A-25})$$

The *Total Current Harmonic Distortion*, *distortion factor* and *displacement power factor* are shown in equations (A-26), (A-27) and (A-28).

$$THD_I(A, B, \phi) = \frac{\sqrt{\sum_{n=2}^{\infty} Ap^2(x, n, A, B, \phi)}}{Ap(x, n=1, A, B, \phi)} \quad (\text{A-26})$$

$$df(A, B, \phi) = \frac{1}{\sqrt{1 + THD_I^2(A, B, \phi)}} \quad (\text{A-27})$$

$$dpf(A, B, \phi) = \cos(\Phi p(n=1, A, B, \phi)) \quad (\text{A-28})$$

The *power factor* is expressed in terms of *displacement power factor* and *distortion factor* as shown in equation (A-29). As was previously identified for *power factor*, equation (A-22) can be expressed in terms of $V_{rms_secondary}$ by using iterative techniques to solve the non-linear equation (A-7) for firing angle ϕ for a given RMS load voltage [29].

$$pf(A, B, \phi) = df(A, B, \phi) \cdot dpf(A, B, \phi) \quad (\text{A-29})$$

Appendix B will utilize the equations derived in this section and associated plots will be generated to verify the results are as expected. Section B.1 will utilize an experimental measurement of a household light dimmer circuit, where the lower voltage tap is set to 0 volts in the math model. Section B.2 will utilize an intuitive approach for known relationships regarding voltages and power to verify the *power factor* for the case of multiple taps. It should be noted that the equations derived in this section can be utilized for any number of transformer secondary taps. Each region between a pair of taps consists of a lower voltage tap and an upper voltage tap. A plot for the entire range of secondary voltages combines the equations applied for each specific region. Appendix C uses the equations for phase displacement of the fundamental and higher order harmonics to specifically investigate the effect of harmonic cancellation.

APPENDIX B- EXPERIMENTAL MEASUREMENTS AND MATH MODEL VERIFICATION

This section investigates the model developed in Appendix A to verify the model predictions for *power factor*. Section B.1 evaluates the case of the lower tap voltage set to 0 volts ($A=0$), such as is the case for a household light dimmer circuit. Controlling the voltage in such a manner from an upper tap down to zero is commonly referred to as *phase angle* control. For using a pair of transformer taps, an intuitive approach is provided in section B.2 where known conditions at half power in phase angle control are utilized to show that the math model provides the expected results.

B.1 Math model verification for lower voltage tap set to 0 volts (i.e. light dimmer)

An experimental setup and Fluke 43B Power Quality Analyzer was used to compare the developed math models and an actual light dimmer circuit. As was noted, the only difference between the light dimmer example and those using a pair of transformer taps is that the lower voltage tap was set to a value of 0 for the light dimmer example, effectively functioning as a single tap. The experimental set-up is shown in Figure B-1.

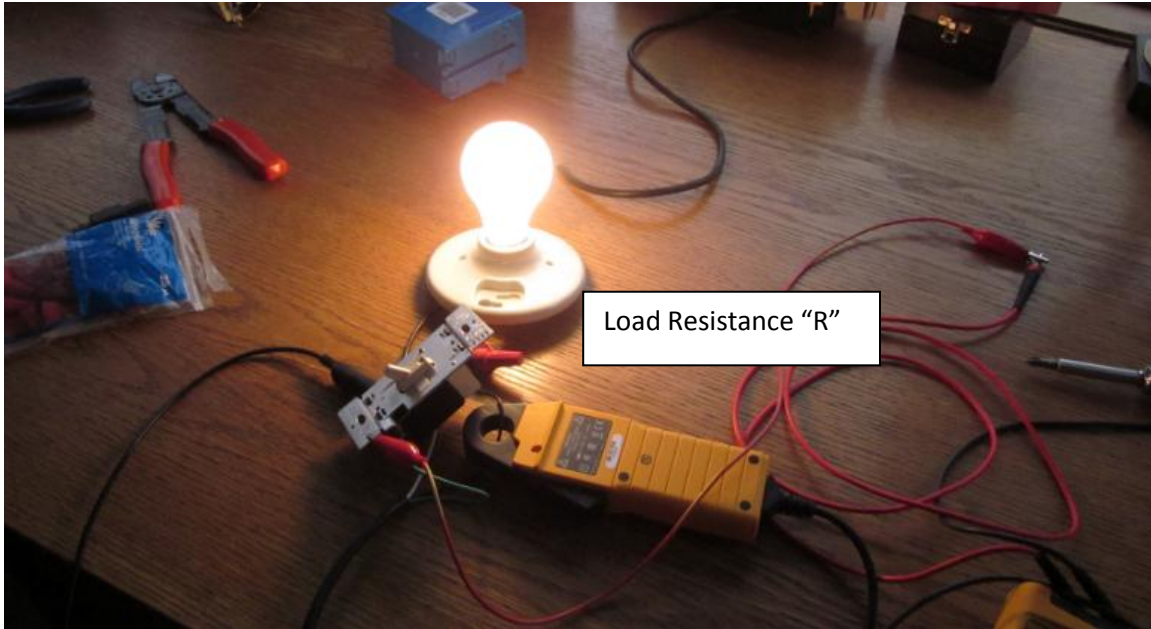


Figure B-1: Experimental light dimmer setup

Shown in Figure B-2 is a plot of the supply voltage of 118.5 volts and the load voltage at 84.9 volts for approximate 90 degree firing (half power) [8]. Using the math models developed in Appendix A, it can be seen from the plot in Figure B-4 the *power factor* linearly decreases from 1 to 0 when the voltage varies from the nominal tap voltage of 120 volts down to 0 volts. Utilizing the linear relationship, the *power factor* for the experimental set-up should be $84.9/118.5=0.716$. Figure B-3 shows the measured *power factor* to be 0.72, very closely matching the value identified from the math model ~0.72.

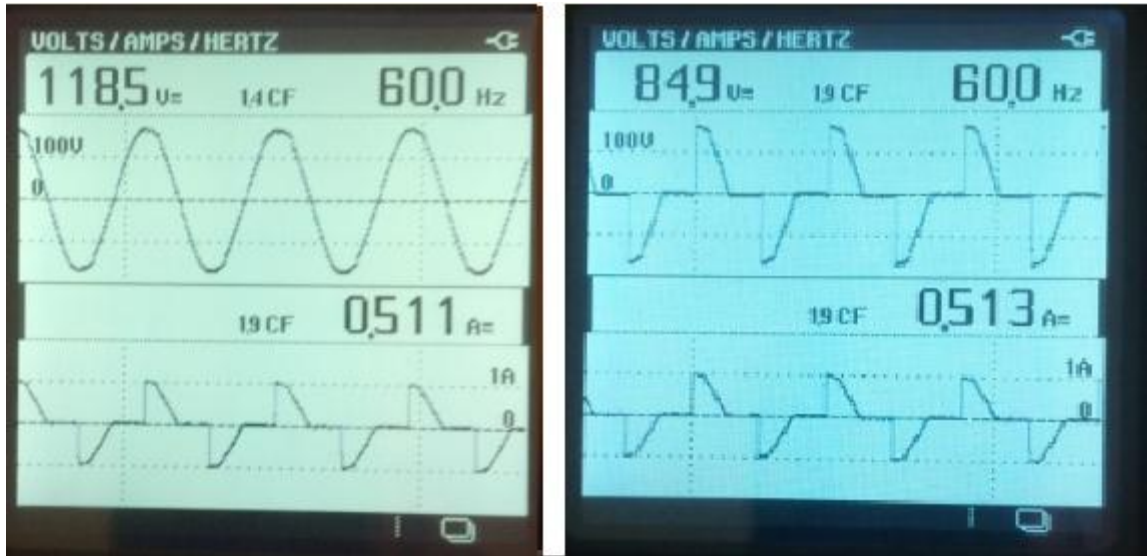


Figure B-2: Supply current / voltage and load current / voltage

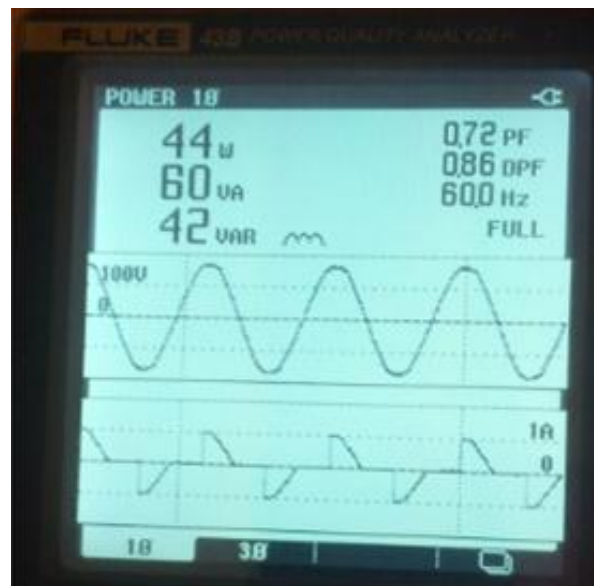


Figure B-3: Power factor for the dimmer half dimmed (90 degree firing)

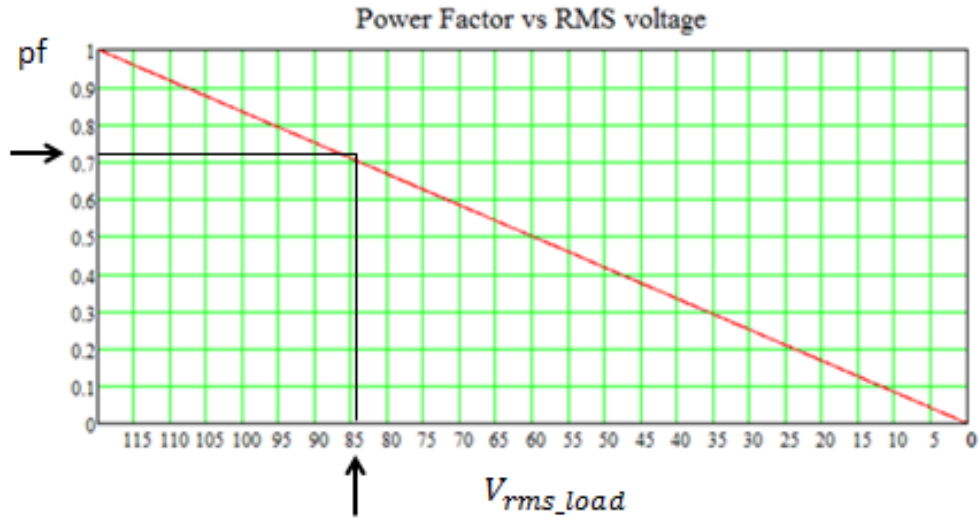


Figure B-4: Light dimmer plot of power factor vs. RMS voltage

It should be noted that when half the waveform is applied for half power and using 120 volt supply, the RMS voltage of half the wave is $120/\sqrt{2} \sim 85$ volts [8]. For a resistance “R”, the power can be shown to be $(120/\sqrt{2})^2/R = (1/2)(120^2/R)$ or half power for a given resistive load. The result will be used in the subsequent analysis for validating the math model when a second transformer tap is used.

Further verification from the math model is obtained by plotting the *displacement power factor* and *distortion factor* components of *power factor* to show that the results are consistent with those expressed as a function of RMS voltage. The first graph shown in Figure B-5 shows an applied voltage with an arbitrary peak amplitude of 1, the secondary waveform and the fundamental component at 90 degree firing. The peak amplitude of the voltage could have been any value as it does not have an impact on the *power factor* or *harmonic distortion*.

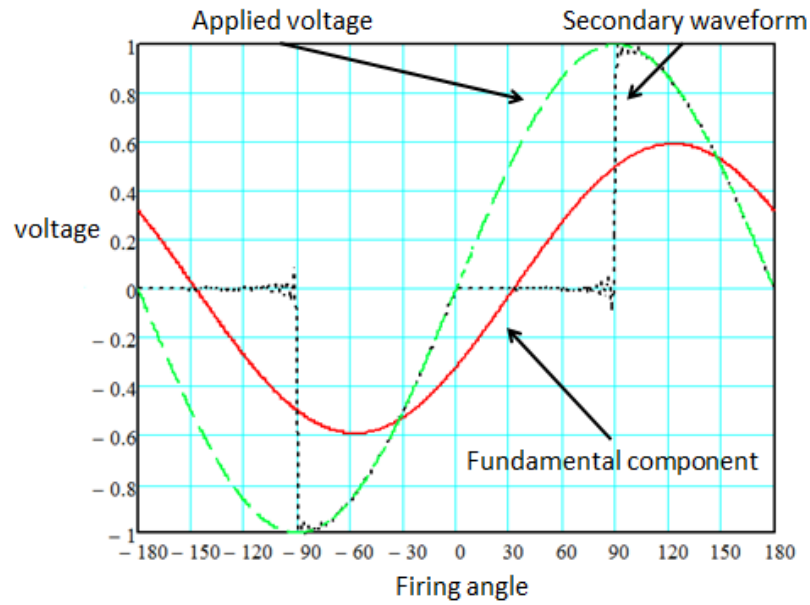


Figure B-5: Applied voltage, secondary waveform and fundamental harmonic

A plot of the *displacement power factor* vs. firing angle is shown in Figure B-6 and *distortion factor* in Figure B-7. Additionally, a plot combining both *displacement power factor* and *distortion factor* shows the *power factor* in Figure B-8. It can be seen that at 90 degree firing angle, the *power factor* matches closely with the plot vs. RMS voltage as well as that measured experimentally.

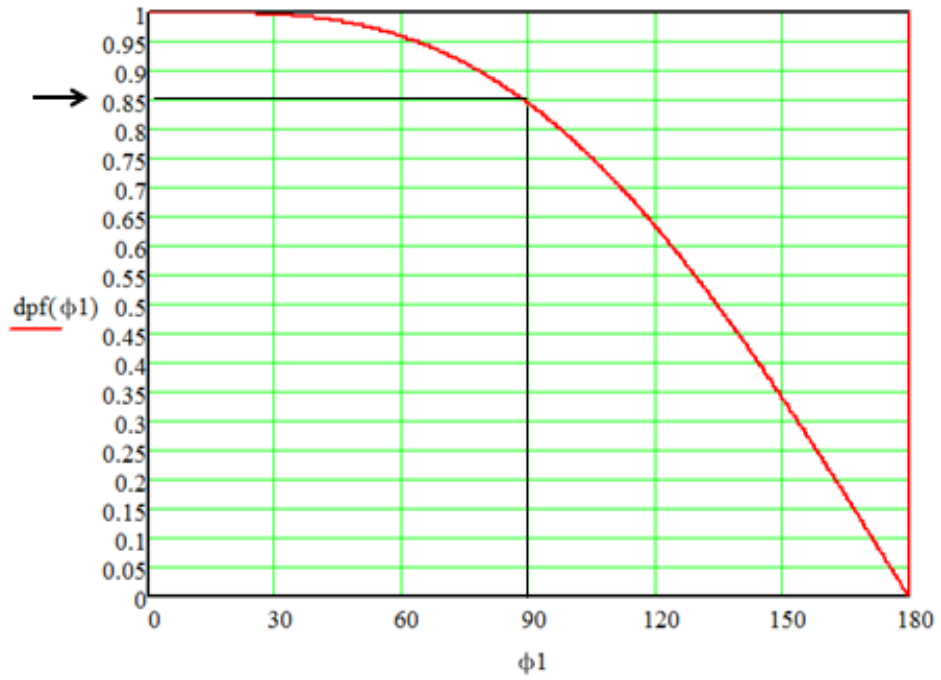


Figure B-6: Displacement power factors vs. firing angle

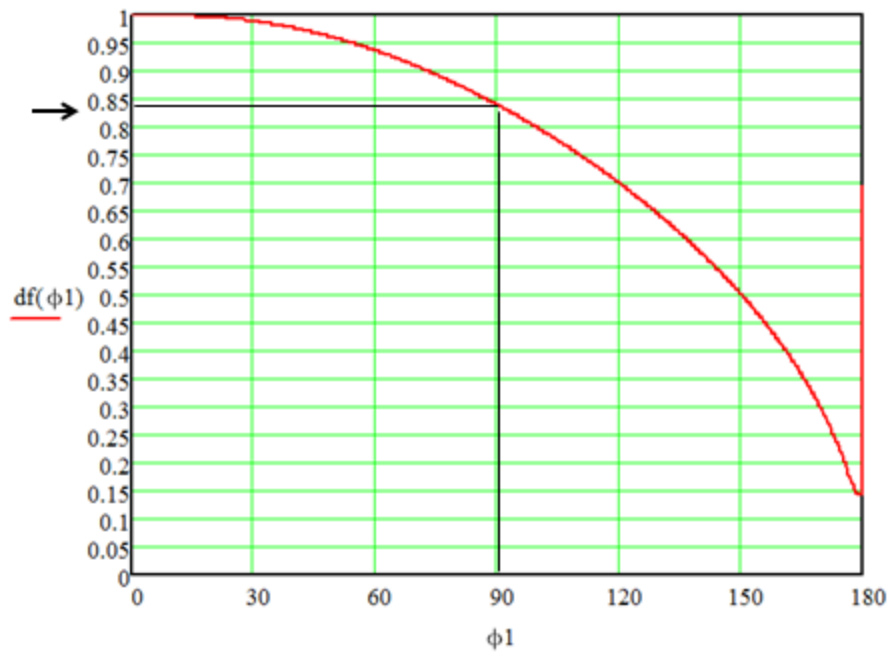


Figure B-7: Distortion factor vs. firing angle

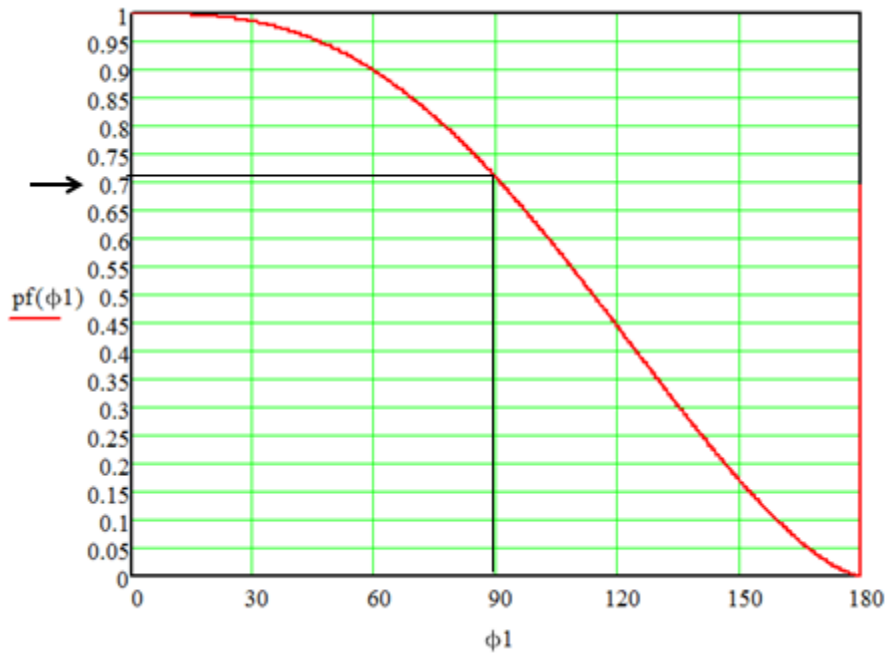


Figure B-8: Power factor vs. firing angle

B.2. Math model verification for operation between a pair of transformer taps

To verify *power factor* for the condition operating between a pair of voltage taps, nominal RMS voltage taps of 60 and 120 volts will be used for the secondary and a primary voltage of 120 volts. The circuit and corresponding voltage waveform at 90 degree firing is identified in Figure B-9. The plot of *power factor* vs. RMS voltage is shown in Figure B-10. Since a light dimmer does not provide the ability to test *power factor* using multiple taps and industrial sized power supplies are expensive and not readily available for testing, an alternate approach is applied to verify the math model at 3 points to provide a strong level of confirmation of the model results.

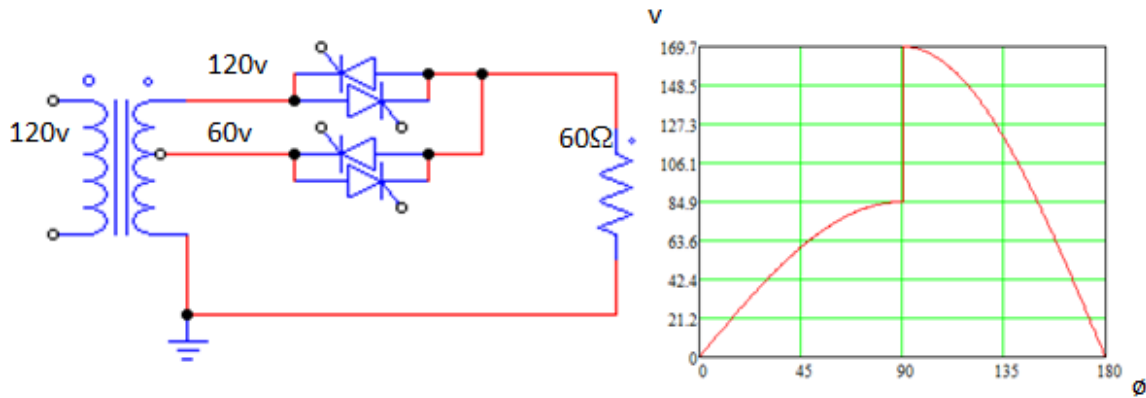


Figure B-9: Load voltage for 90 degree firing between 60 and 120 volt taps

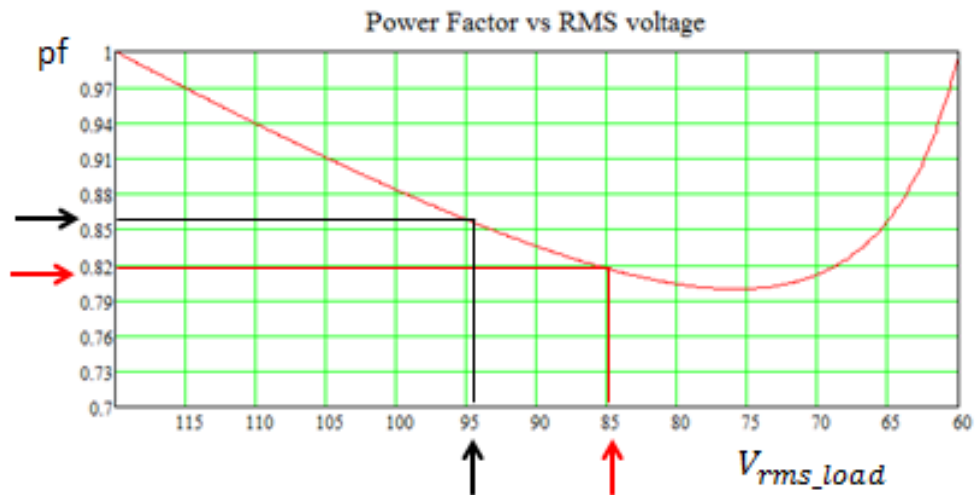


Figure B-10: Power factor vs. RMS voltage operating between 60 and 120 volt taps

It is known that the *power factor* must be 1 at both extreme ends of the nominal voltage taps (60 and 120 volts) since the voltage will be sinusoidal at those points. For the third point of confirmation, the information known about applying half the wave (90 degree firing) and half power is utilized (see section B.1). It was identified that the RMS value for half the wave applied was the RMS value of the full wave divided by $\sqrt{2}$. If using phase fired SCRs to control the voltage to the load as is shown in Figure B-9, it

would be expected to have a current of $1 A_{rms}$ to the 60Ω load if 180 degree firing were used (never switching from the 60 volt tap to the higher voltage tap). Applying the 60/120 transformer turns ratio, the corresponding primary current would be $0.5 A_{rms}$. On the other hand, if 0 degree firing angle were used (immediately switching to the higher voltage tap of 120 volts), the load current would be $2 A_{rms}$ as would the primary current since the transformer turns ratio would be 120/120. Based on what was identified relative to the RMS value when half the waveform is applied (90 degree firing), the corresponding RMS currents for the primary and secondary of the transformer are shown in Figure B-11. It should be noted that the different RMS values shown only apply to half of the waveform (0-90 degrees or 90-180 degrees respectively) and not the total RMS for a cycle. Both quantities must be combined to compute the total RMS current.

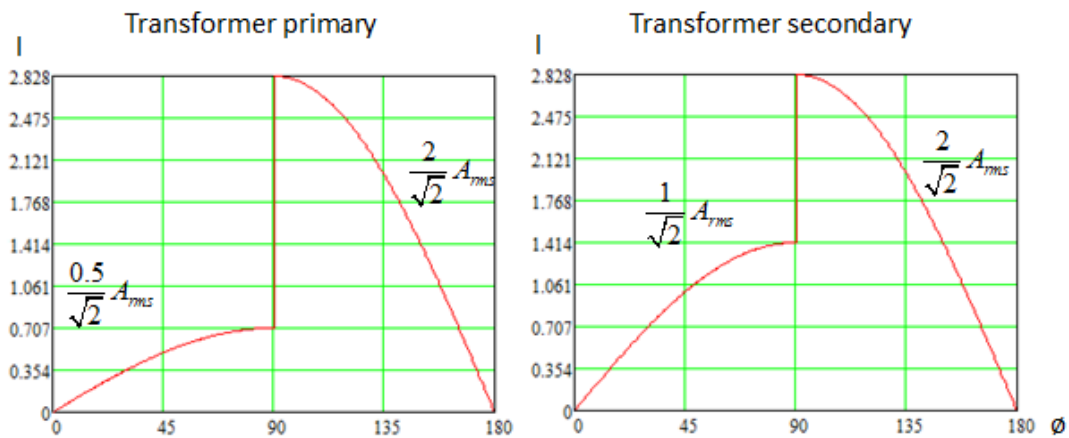


Figure B-11: Transformer primary and secondary currents for a 60 ohm load

The total RMS current for the primary and secondary are calculated as shown in equations (B-1), (B-2) and (B-3) which are direct results from applying the equation defining an RMS quantity [4]. Additionally, the RMS load voltage is also calculated.

$$\sqrt{(0.5/\sqrt{2})^2 + (2/\sqrt{2})^2} = 1.46A_{rms} \quad (B-1)$$

$$\sqrt{(1/\sqrt{2})^2 + (2/\sqrt{2})^2} = 1.58A_{rms} \quad (B-2)$$

$$\sqrt{(60/\sqrt{2})^2 + (120/\sqrt{2})^2} = 94.9V_{rms} \quad (B-3)$$

The RMS quantities are utilized to calculate the power at the load, primary *apparent power* and corresponding *power factor*. The *power factor* is calculated to be 0.86 matching that shown in the math plot in Figure B-10 for the load voltage of 94.9 volts.

Table B.1: Voltage, current, apparent power and power factor

Primary			Secondary				
V	I	S	V	I	IR (Calc.) V	P	pf
120	1.46	(120)(1.46)=175.2	94.9	1.58	(1.58)(60)=94.9	(1.58) ² (60)=149.8	149.8/175.2= 0.86

APPENDIX C - HARMONIC CANCELLATION

In section 2.2, an industrial process was analyzed to improve voltage tap spacing for a 3 tap transformer secondary to maximize average *power factor*. The system is again shown in Figure C-1.

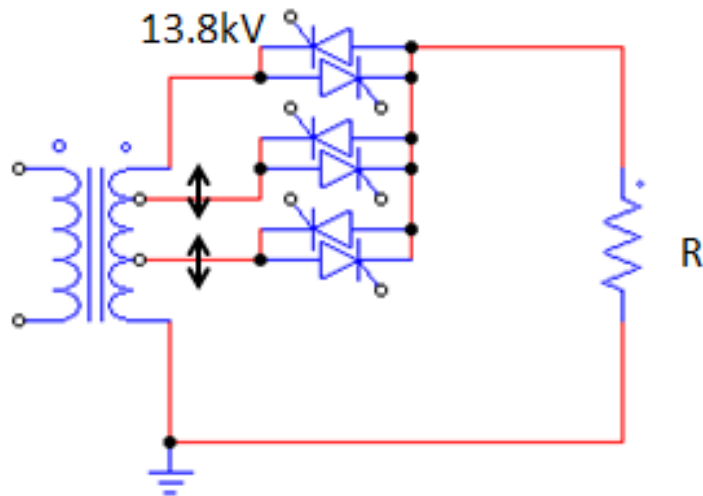


Figure C-1: Transformer supplying an industrial load for process heating

It was identified that the *displacement power factor* was chosen to be optimized rather than *true power factor* which includes the *distortion factor* component. Although the *distortion factor* creates a significant contribution to reduced *power factor* of a single system, it was identified that many loads operated from a bus will often have harmonic cancellations that result in the net *distortion factor* being a negligible contribution to plant *power factor* [30, 31, 32]. Figure C-2 shows an industrial bus with 8 different loads

being supplied by transformer and associated power electronics are contained in a *switch mode power supply* (similar to the SCRs and electronics of a light dimmer being housed in the dimming device).

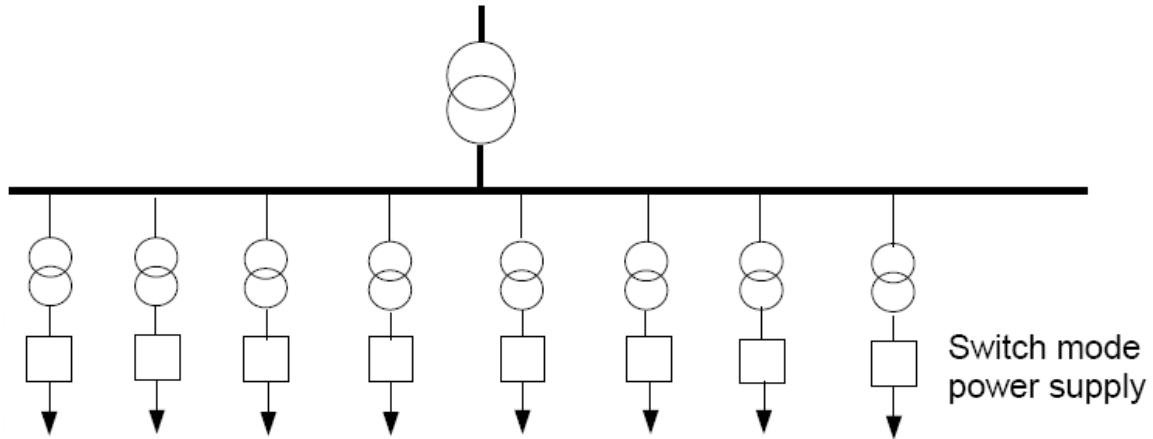


Figure C-2: Industrial bus with several converter power supplies

The equations developed for the load voltage and current from Appendix A were re-arranged in their polar form and are also identified in that section. The polar representation is utilized to plot phase shift vs. firing angle which is necessary for understanding why a reduction in THD and corresponding *distortion factor* is likely to occur for a plant with many systems operating.

For a fixed pair of tap voltages, a plot of the fundamental harmonic vs. firing angle (from 0-180 degrees) is shown in Figure C-3. As can be seen from the plot, the maximum phase shift is approximately 30 degrees lag from the applied voltage for a 120 degree firing angle.

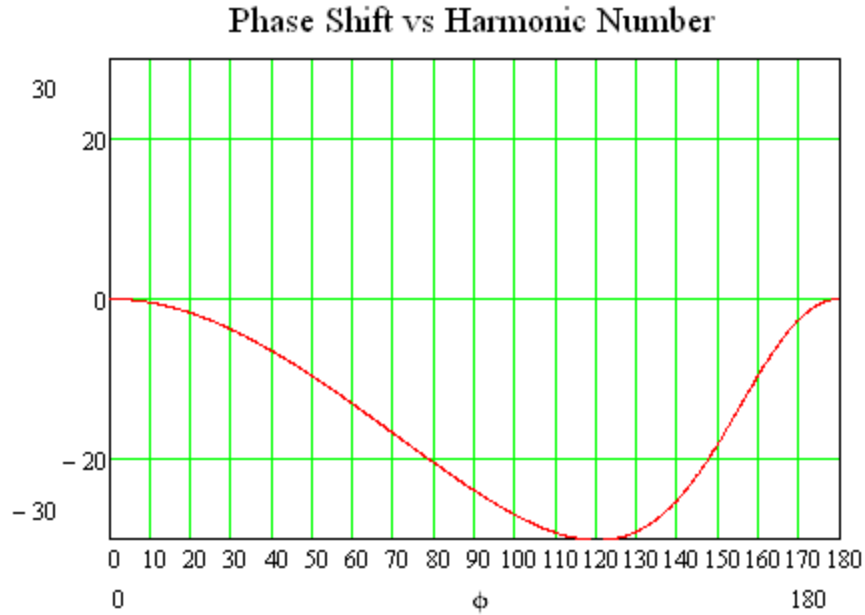


Figure C-3: phase shift of the fundamental harmonic

A plot of the 3rd harmonic is shown in Figure C-4 and it can be seen from the corresponding plot that a much larger range of phase orientation occurs over the full range of voltage between the pair of transformer taps (varying the firing angle from 0-180 degrees). A time domain plot Figure C-5 helps to better interpret the total phase displacement that occurs over the range of applied voltage. From reviewing the time domain plot, it can be seen that the 3rd harmonic phase shift rotates through an angular phase displacement of 360 degrees (relative to the voltage) when the firing angle is also varied from 0-180 degrees.

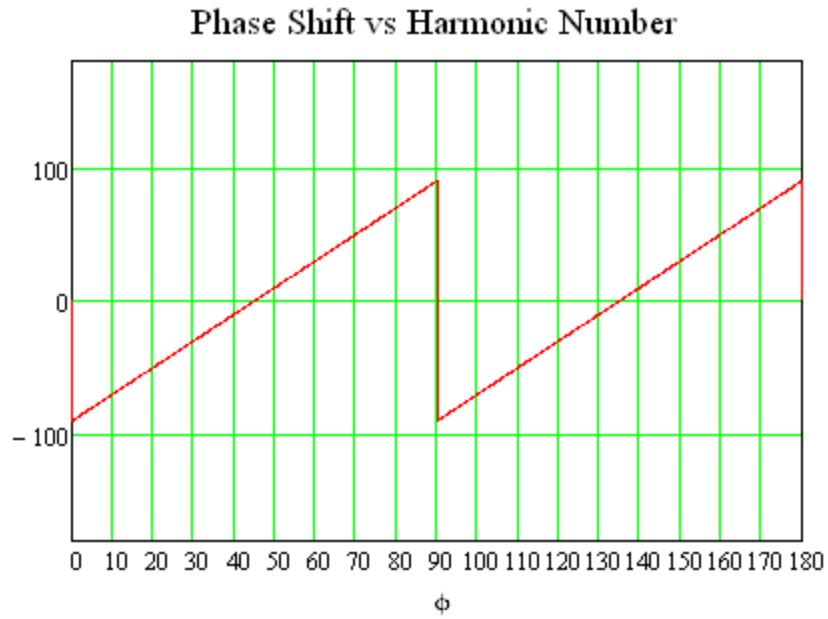


Figure C-4: 3rd harmonic phase shift

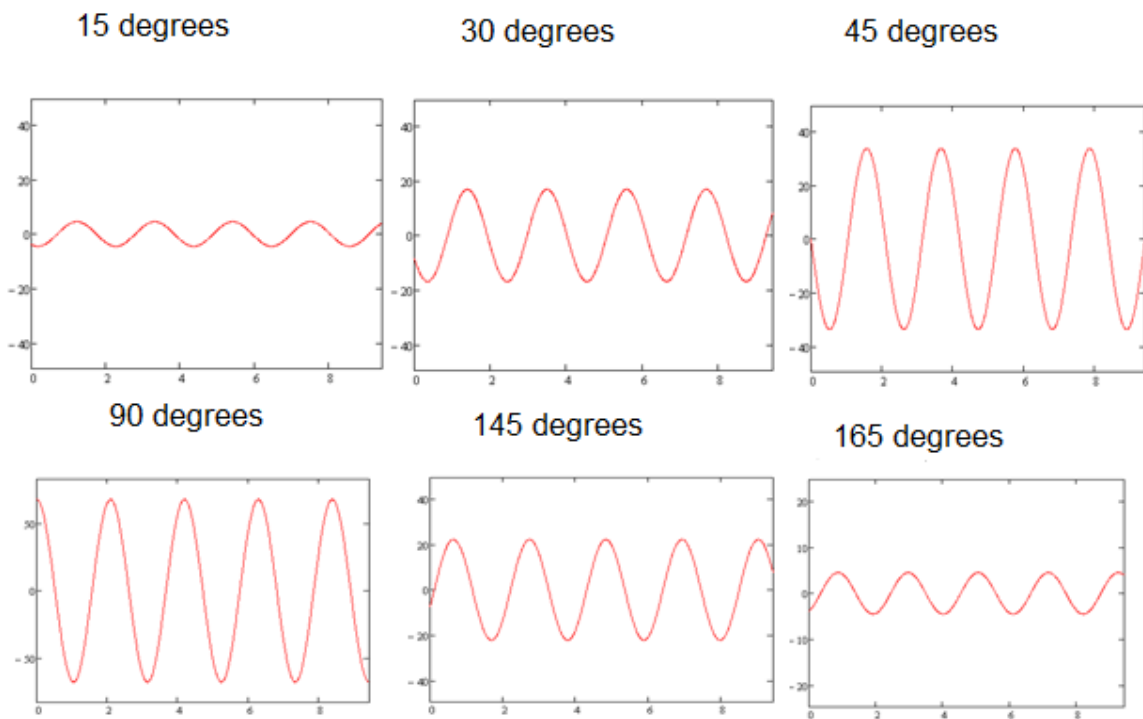


Figure C-5: 3rd harmonic time domain for various firing angles

A phasor plot of both the fundamental harmonic and the 3rd harmonic is shown in Figure C-6 for the range of firing angles to help interpret the plots from Figure C-3, Figure C-4 and Figure C-5. It must be noted that the amplitudes of the phasors shown in the plot is not representative as the 3rd harmonic will have a length/amplitude of 0 when at either 0 or 180 degree firing. The phasors are only shown to identify their orientation to understand the origin of harmonic cancellations. It can be seen that there is much greater range of possible 3rd harmonic phase displacement from the original applied voltage source compared to that of the fundamental harmonic. When multiple systems are operating on a bus, the corresponding harmonic components of one system will add as phasors with those of the other systems. Since the fundamental component is approximately in phase (maximum of 30 degrees from the applied voltage) for systems at different firing angles (but same tap spacing), the combined fundamental components will approximately add algebraically regardless of each individual system's voltage applied to the load. The net 3rd harmonic components on the other hand, will not increase as dramatically due to their phasor orientations. An example of two systems operating at different voltages corresponding to 45 and 90 degree firing is used to further explain the concept. For the combined systems, the net fundamental component will approximately double (assuming equal current magnitudes for both systems). Assuming equal magnitudes, the 3rd harmonic component for both systems will only increase by a factor of $\sqrt{2}$ (since their current phasors will have a 90 degree displacement from each other).

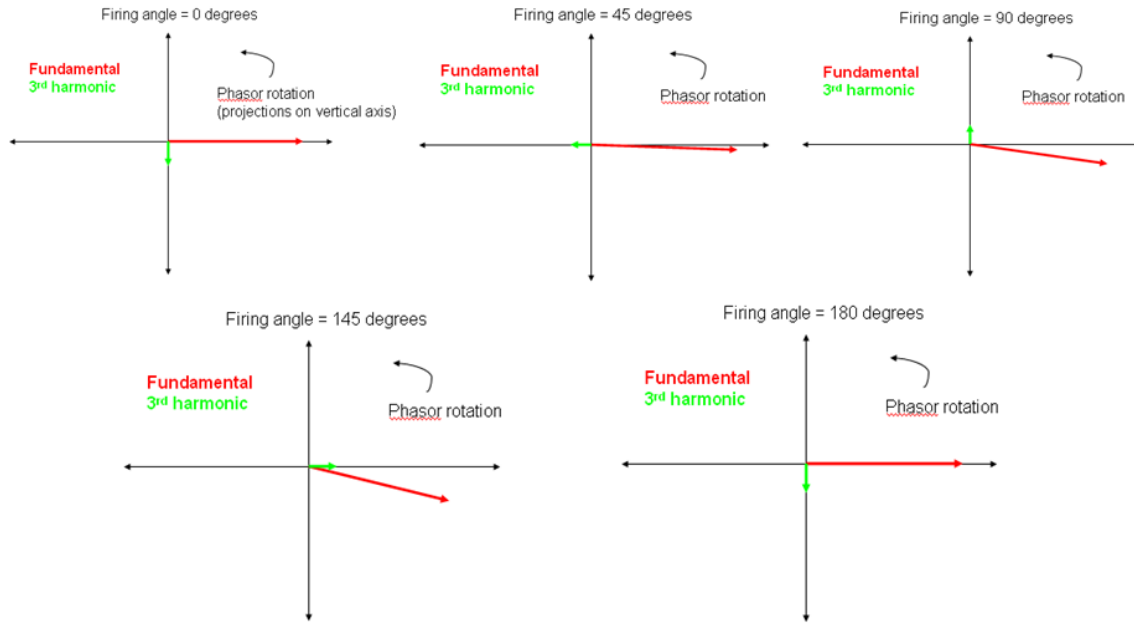
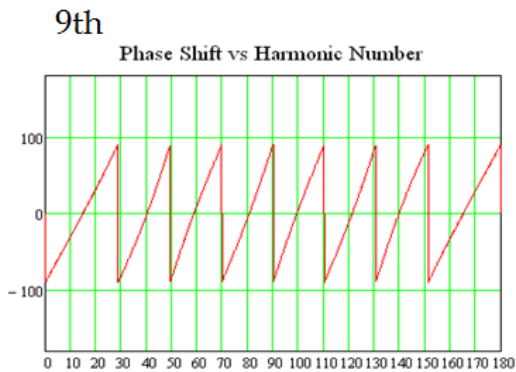
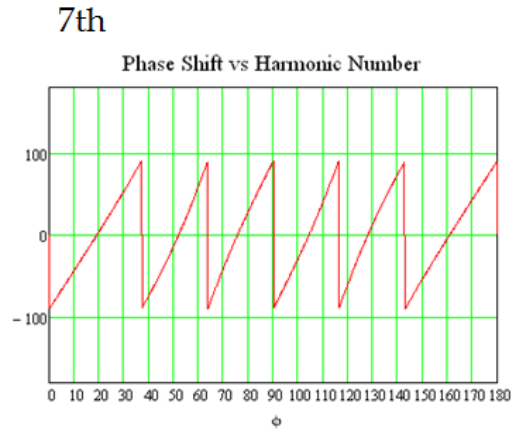
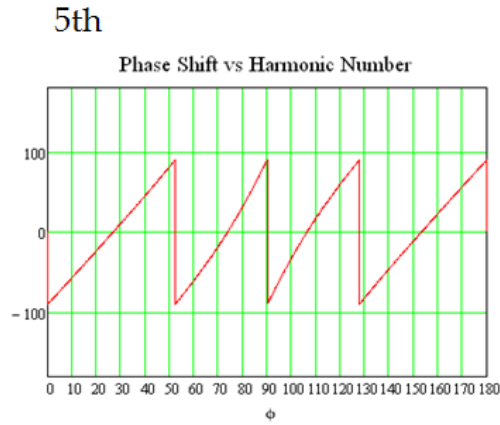


Figure C-6: 3rd harmonic and fundamental phasor displacement vs. firing angle. Note: different harmonics have a different angular speed of rotation

The next example of phasor plot compares the 5th, 7th and 9th harmonics. This plot in Figure C-7 shows that the higher order harmonics have a much larger range of displacement for a fixed range of firing angles (varying process voltage). In general, when the process voltage is varied over the full range between a pair of voltage taps (0-180 degree firing angle), it can be seen that the range of possible phasor displacement from the applied voltage for harmonic components beyond the fundamental is $(n-1)(180$ degrees), where n is the harmonic order (i.e. 3rd, 5th, etc.).



General Relationship
(phasor rotation for varying
firing angle 0-180 degrees)

$$(n-1)(180 \text{ degrees})$$

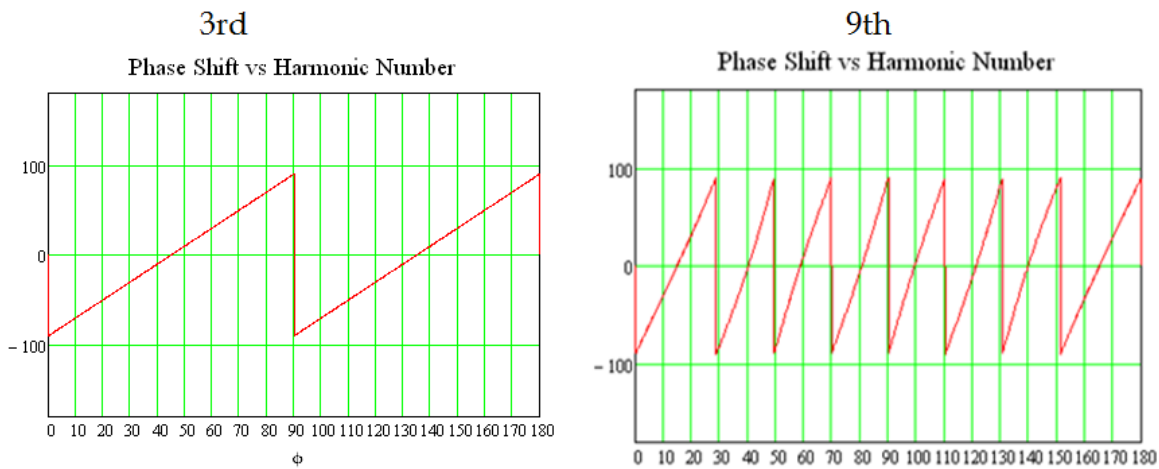
Figure C-7: 5th, 7th and 9th phase shift

A closer look at comparing the 3rd and 9th over a fixed firing angle range (90-110 degrees) is shown in Figure C-8. The figure shows that the 9th will have possible phasor displacement of up to 180 degrees whereas the 3rd will have a much smaller displacement. Two almost identically controlled loads at 90 and 110 degree firing angle would exactly cancel the 9th harmonic and only partially cancel the 3rd harmonic (once again assuming equal current magnitudes for each system for harmonics of the same order). For two systems operating at 90 and 110 degree firing angle, there will not be a substantial difference in their output voltages and corresponding powers (assuming the same load resistance), however. Therefore, even for systems on a bus that are at

similar operating points, higher order harmonics will tend to have a higher probability of cancelling for the combined system.

This general relationship can best be understood by thinking of expected value for various outcomes with a given probability [31]. Higher order harmonics will have a higher probability of cancellation for a fixed range of firing angle due to the larger number of possible orientations.

$$E = \sum V_i p_i \text{ where } V_i \text{ is a value with probability } p_i$$



Compare between 90-110 degrees for instance

Figure C-8: 3rd and 9th phase shift vs. firing angle

Figure C-9 and Figure C-10 are used to graphically show the additive effects that occur for the fundamental and 3rd harmonic components of 3 systems operating. Since the relative amplitudes of the fundamental current will increase at a greater rate than the higher order harmonic components, it can be seen from equation (C-1) that the *THD* must decrease for the combined system.

$$THD_I = \frac{\sqrt{\sum_{n>1}^{n_{max}} I_n^2}}{I_1} \quad (C-1)$$

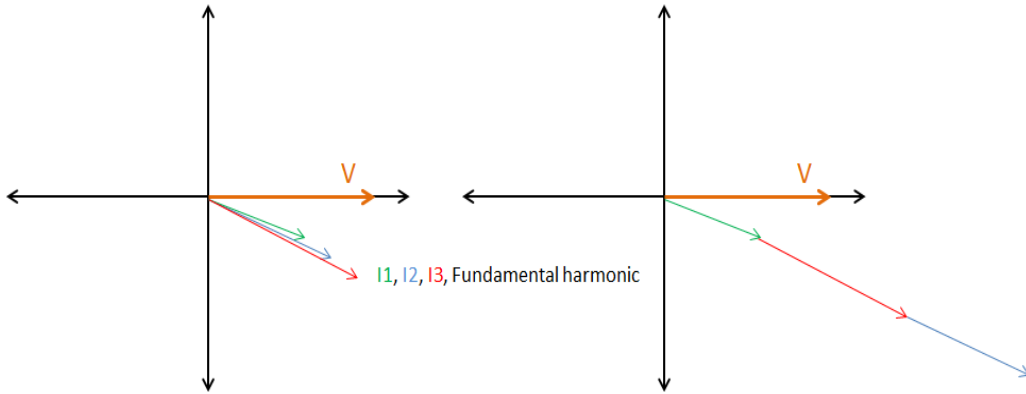


Figure C-9: Fundamental harmonic components for 3 systems

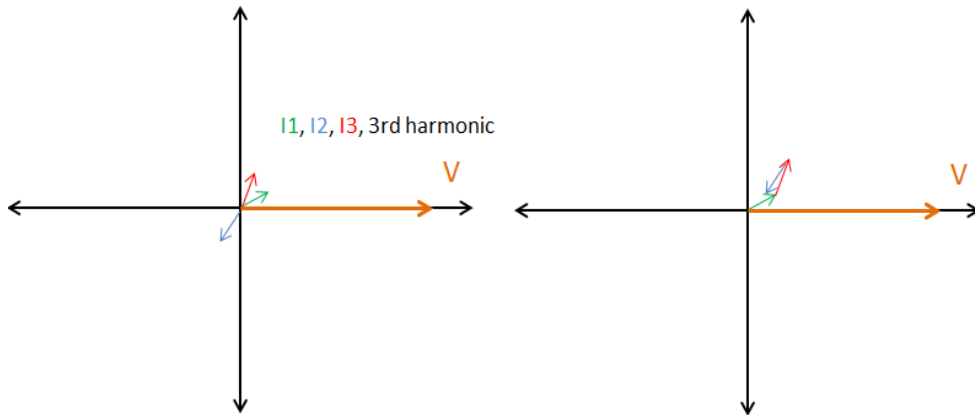


Figure C-10: 3rd harmonic component cancellation for 3 systems

In Appendix A, it was shown that the primary current waveform is of the form shown in Figure C-11. For power distribution systems, it is common for the transformer to be connected in a delta/Y (primary/secondary) configuration [13, 17]. A delta connected transformer primary, the waveform shown is the phase current and the line current must be computed as the phasor subtraction of the corresponding phase currents. For a positive a, b, c phase sequence, the line current for the a phase can be expressed as $I_L = I_{ab} - I_{ca}$ [19].

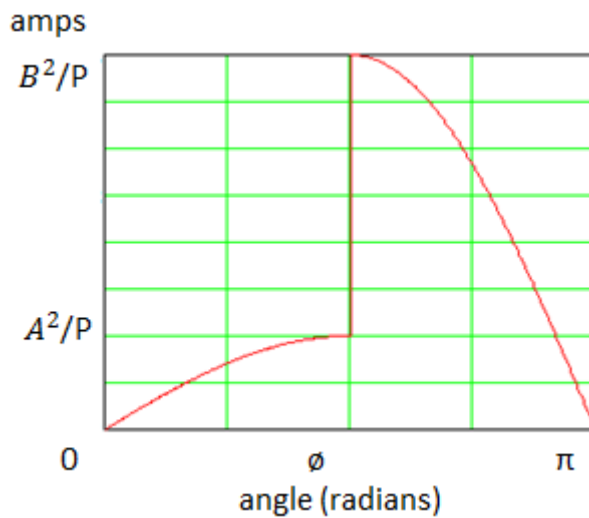


Figure C-11: Delta connected primary phase winding current waveform

The phasor subtraction of current for the loads controlled by each phase of the transformer creates some level of harmonic cancellation before being added to other systems. An example simulation of the line currents of 3 systems operating in a slightly unbalanced condition is shown below in Figure C-12 as well as the total line current to help show the visual reduction in distortion of the combined system. The sum of the total line current is less distorted (more sinusoidal) than any of the individual systems.

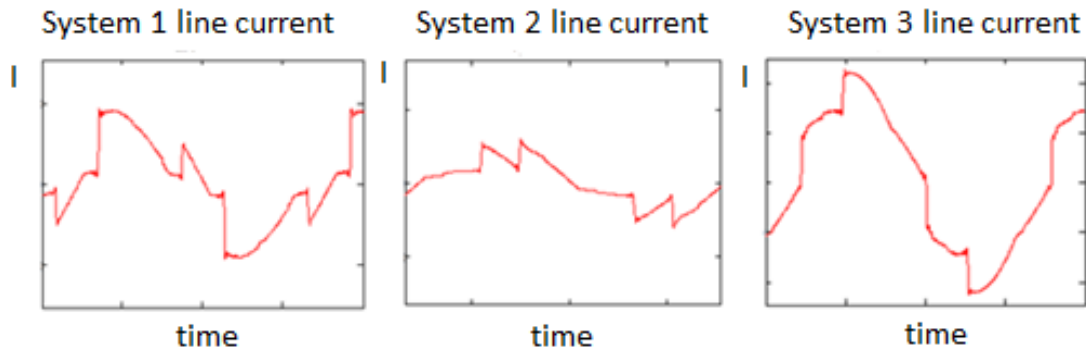


Figure C-12: Line currents for 3 systems simulated

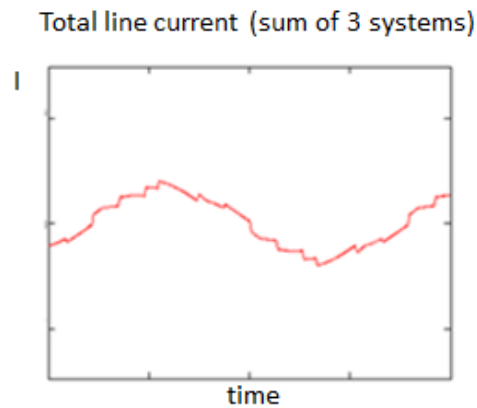


Figure C-13: Sum of the line current for 3 systems

As was previously identified, an industrial bus with a THD_I of 10%, the *distortion factor* is only $df = 0.995$, a small contribution compared to the *dpf*. A plant with many systems operating may have a net THD_I such that the *distortion factor* becomes negligible. The designer must apply their knowledge and understanding of the system to determine the best approach to apply during the optimization procedure.